May 2020

A Tale of Two Adaptors: the Role of Two Adaptor Proteins in Pseudomonas Aeruginosa CHP Chemosensory System Signal Transduction and Implications for Chemosensory Array Formation

Zachary Hying
University of Wisconsin-Milwaukee

A TALE OF TWO ADAPTORS: THE ROLE OF TWO ADAPTOR PROTEINS IN *PSEUDOMONAS AERUGINOSA* CHP CHEMOSENSORY SYSTEM SIGNAL TRANSDUCTION AND IMPLICATIONS FOR CHEMOSENSORY ARRAY FORMATION

by

Zachary T. Hying

A Thesis Submitted in

Partial Fulfillment of the

Requirements for the Degree of

Master of Science

in Biological Sciences

at

The University of Wisconsin-Milwaukee

May 2020

ABSTRACT

A TALE OF TWO ADAPTORS: THE ROLE OF TWO ADAPTOR PROTEINS IN *PSEUDOMONAS AERUGINOSA* CHP CHEMOSENSORY SYSTEM SIGNAL TRANSDUCTION AND IMPLICATIONS FOR CHEMOSENSORY ARRAY FORMATION

by

Zachary T. Hying

The University of Wisconsin-Milwaukee, 2020
Under the Supervision of Professor Sonia L. Bardy

Bacteria use chemosensory systems to coordinate environmental signals to direct chemotaxis and make lifestyle decisions such as surface attachment and biofilm formation. Chemosensory systems form extended arrays with pseudo-hexagonal symmetry that are essential for efficient signal transduction. These arrays consist of three essential components: Methyl-Accepting Chemotaxis proteins (MCPs), which receive signals, a histidine kinase to coordinate cell responses through phosphorylation of response regulators, and an adaptor protein to transduce conformational change and facilitate array formation. *Pseudomonas aeruginosa* uses four chemosensory systems to control flagellar-based motility, type IV pili-mediated twitching motility and acute virulence, and biofilm formation. The Chp chemosensory system regulates two outputs: direct actuation of type IV pili supports twitching motility, and modulation of intracellular levels of cyclic-AMP (cAMP) regulates pilus biogenesis and acute virulence. In the Chp chemosensory arrays conformational changes are transduced from a single MCP, PilJ, to the histidine kinase, ChpA, via two adaptor proteins, PilI and ChpC.

Using molecular techniques, we determined functional roles for PilI and ChpC. Our results show that PilI is essential for signal transduction and can facilitate twitching motility without ChpC in the presence of excess cAMP. ChpC serves as a cooperative adaptor for signal

amplification necessary for efficient modulation of intracellular cAMP levels. We also investigated the interactomes of each adaptor and found that PilI and ChpC interact with each other, but curiously, neither PilI nor ChpC can self-interact. Additionally, our findings suggest PilI is the only adaptor protein that can interact with the histidine kinase ChpA.

Based on the interactomes and functional roles of PilI and ChpC, and the known universal architecture of chemosensory arrays, we constructed a model for Chp chemosensory array formation. This study develops a method to understand and predict chemosensory array formation in lieu of directly visualized structural data and could be used to better understand how other chemosensory systems that incorporate multiple adaptor proteins function. This study also offers insight into Chp system function and suggests multiple potential avenues for further study.

TABLE OF CONTENTS

LIST OF FIGURES

LIST OF TABLES

ACKNOWLEDGEMENTS

Grad school has its ups and downs, from days experiments go beautifully, to months were nothing seems to work. Your ideas are sometimes great and worthy of beautiful prose, and sometimes they're just downright non-sensical. But if you don't believe in yourself and your science, you may end up like those who shout nonsense towards the ivory tower, for science enlightens us, even in a lab without fenestration, instead of keeping us locked away in the caves of dogmatism. This spring I graduate, naïve and hopeful, despite the outside world looking so grim. And now, as I look forward unto the world, I see innumerable possibilities, but none shall come to pass if we shout instead of listen. For science wants to bring us up, while the confused and fanatical drag us down. In short, this is now, and I insist on being received, but only to be discussed amongst my peers, for the best for us all.

Now, to digress from Dickensian prose, I must first thank my scientific parents. Dr. Sonia Bardy for being a stalwart advisor whose advice, understanding and scientific mind I aspire to. Dr. Mark McBride for the trust you placed in me, and the freedom I received despite a lack of significant experience. And, Dr. Gyaneshwar Prasad for giving me my first research opportunity and helping me get my toes wet in the vast scientific world.

Second, I must thank my biological parents, Clem Hying and Val Bogan, for raising me, and supporting me through all the ups and downs that have brought me here. Particular praise is owed to my Mom for always thinking I should pursue a career in science, I am truly here because of you.

Third, I must thank my scientific Aunts and Uncles. Specifically, Dr. Sergei Kuchin, for the excellent assistance with statistics. And Dr. Daad Saffarini, for the use your SDS-PAGE

equipment, your transilluminator, and permission to finish my last experiment during COVID-19 shutdown.

Fourth, I must thank my scientific siblings. Dr. Katherine Affeldt, for the infinite wisdom of being emotionally detached from your results. Dr. Yongtao Zhu, for your mentorship and for passing off a really cool project. And last, Kayla Simanek, for being my partner and equal during our time in the Bardy lab.

Fifth, I must thank my biological siblings. Skyler Hying, for never doubting that I was capable of doing something even though you saw me when times were most bleak. And, to Bryce and Sydney for inspiring me to make this world a better place for you as you approach adulthood.

Sixth and finally, I must thank my chosen family. My chosen sisters Jen Sturchio, and Alysha Rendflesh for always being there when I needed a lift and for making life seem so much lighter than it actually is. And, my chosen brothers of Gunners FC for providing a place where I could decompress from the stresses of school.

Introduction

Bacterial chemotaxis and chemosensory systems

Chemotaxis is the process that motile bacteria and archaea use to bias their movement towards favorable environments or away from unfavorable ones [1]. Chemotactic bacteria do this by sensing an attractant or repellent and transducing a signal via a phosphorylation cascade to control motility [2]. Attractants and repellents are extremely diverse and range from small molecules and oxygen gas, to light and even magnetic fields. Detection and transduction of signals are carried out by a complex of proteins that evolved from bacterial two-component systems and are called chemosensory systems [1].

Chemosensory systems were initially characterized in *Escherichia coli* where chemotaxis is controlled by altering the direction of flagellar rotation [2]. Flagellar chemosensory systems (Fla) are the most well understood chemosensory systems [2]. Two other types of chemosensory systems have been classified; Tfp (type four pilus) chemosensory systems modulate twitching motility, while ACF chemosensory systems regulate diverse alternative cellular functions [1].

All chemosensory systems are two-component-like systems consisting of a sensory complex and a response regulator. The sensory complex consists of three proteins that respond to a signal and initiate a response. The methyl-accepting chemotaxis protein (MCP) is a trans-membrane protein that forms trimers of dimers and localizes to the cytoplasmic membrane. Typically, the periplasmic domain of the MCP binds a signaling ligand, though the transmembrane domains have also been implicated in signal detection [3]. Interaction with a ligand induces conformational changes to the cytoplasmic domains. These conformational changes are transduced by an adaptor protein (CheW) to a histidine kinase homodimer (CheA).

This affects CheA autophosphorylation, which occurs in trans. Phosphorylated CheA transfers the phosphate group to the response regulator (CheY) (Figure 1). In *E. coli* and other Fla chemotaxis systems, phosphorylated CheY binds to the flagellar motor and alters the direction of rotation causing a cell traveling in a relatively straight trajectory (run) to change direction (tumble, reverse, or stall depending on the organism) [2].

Chemosensory array structure and formation

Chemosensory systems exhibit high sensitivity, cooperativity, the ability to fine-tune chemotactic responses and the ability to amplify signal transduction resulting from higher order interactions between multiple sensory complexes that assemble and function together in large ordered arrays [4,5]. The minimal signaling complex of chemosensory systems consists of six homodimers of MCPs arranged as two trimers of dimers. Each receptor trimer of dimers is bound to a monomer of the adaptor protein CheW and one subunit of a histidine kinase dimer CheA. The dimerization domains of CheA interact in between the two receptor trimers (Figure 2A). Multiple core complexes oligomerize into large ordered arrays that have hexagonal and orthogonal symmetry (Figure 2B). The MCP trimers of dimers are regularly spaced at 12 nm intervals within a baseplate consisting of six membered hexagonal rings [6,7]. The architecture of chemosensory arrays is universally conserved among membrane-bound and cytosolic arrays and among bacteria and archaea. [8,9]. Membrane-bound chemosensory arrays often localize to the poles of bacterial cells. In *E. coli* each six membered ring consists of either alternating CheW and CheA or six monomers of CheW [6,10,11]. Dimers of CheA act as structural staples that link one hexagonal ring to another providing structural stability to the array superstructure [10]. The stoichiometry of the baseplate is variable depending on the species, and the fine-tuning of

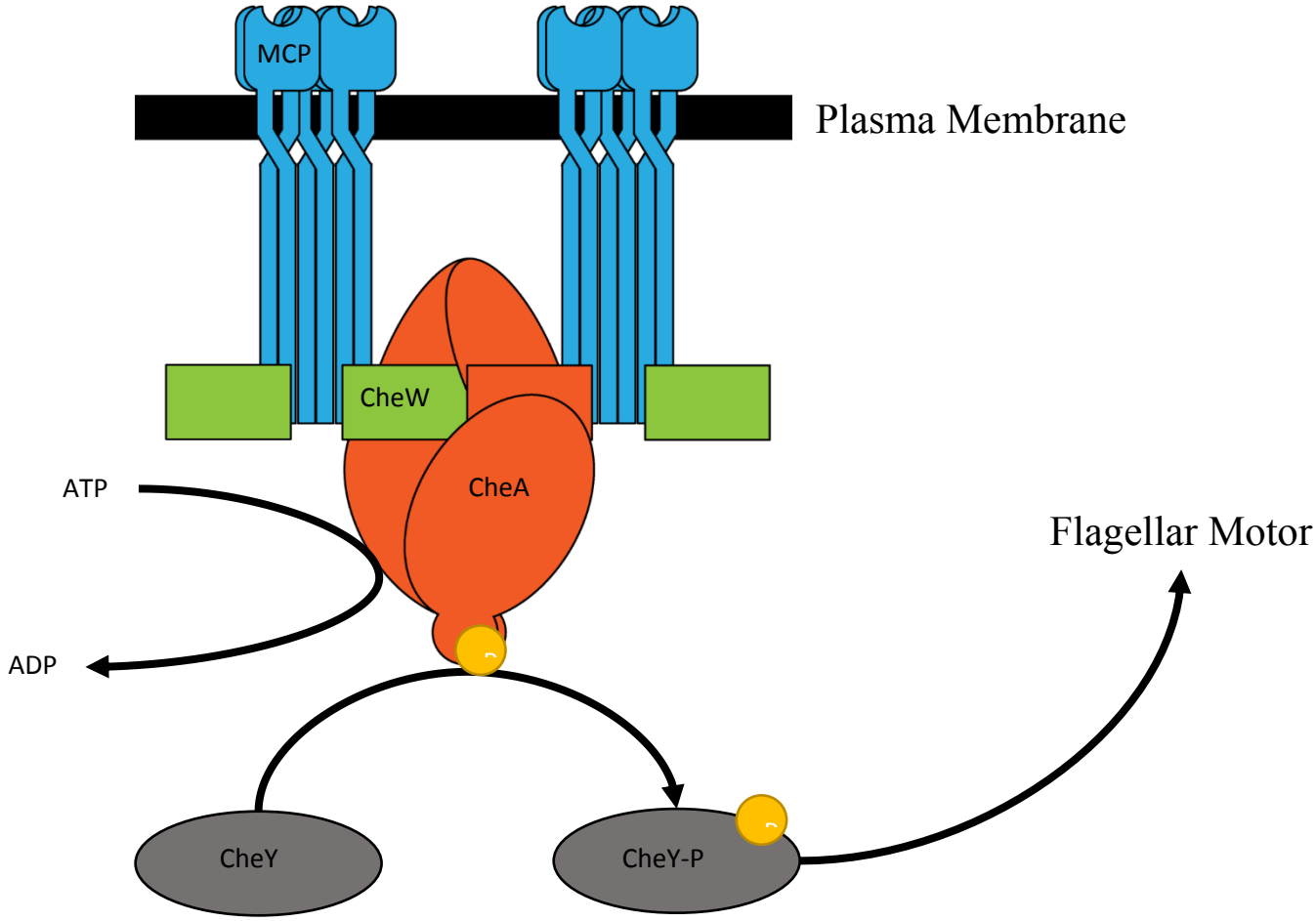

Figure 1 Structure of chemosensory systems. When a signal is sensed by the MCP trimer of dimers a conformational change occurs at the cytoplasmic tip. The conformational change is transduced to CheA via CheW causing autophosphorylation of CheA. CheA-P transfers the phosphate the CheY. CheY-P binds to the flagellar motor to change the direction of flagellar rotation.

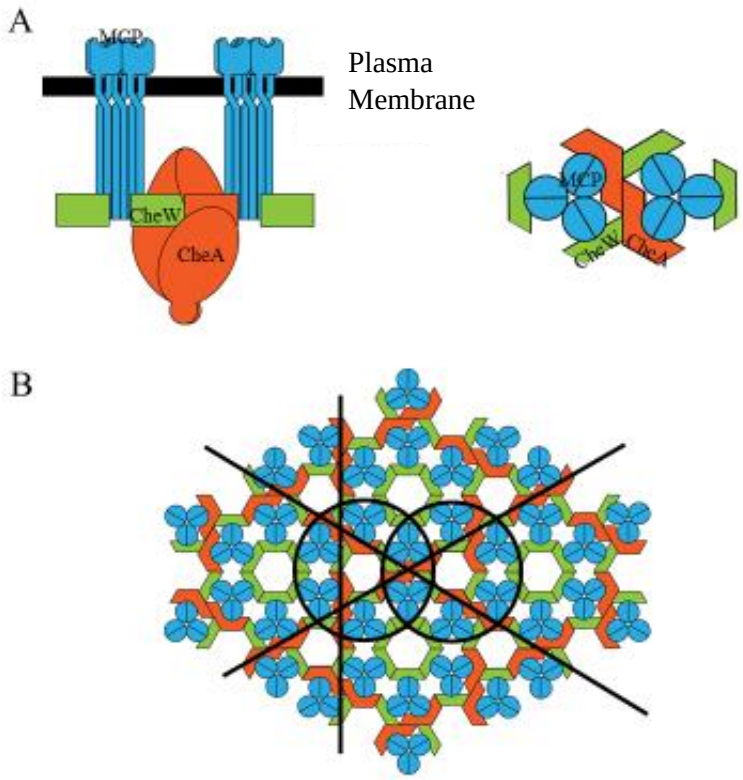

Figure 2 Structure of chemosensory system sensory complexes. A) Shown on left; Side view of a minimal signaling complex showing MCPs embedded in the plasma membrane as trimers of dimers, and cytoplasmic tips interacting with CheW and CheA. Shown on right; Top view of a minimal signaling complex showing MCPs in blue arranged as a trimer of dimers, CheA in orange showing the AIF domain interacting with a dimer of MCPs and the dimerization domain interacting with a second CheA forming a "structural staple". CheW is shown in green interacting with dimers of MCP and with the AIF domain of CheA. B) Top view of an extended chemosensory array as formed through oligomerization of minimal complexes. Circles demonstrate hexagonal symmetry of arrays. Straight lines demonstrate orthogonal symmetry.

chemosensory signaling is dependent on specific stoichiometry of the components that can also vary between species [10]. *E. coli* has a high ratio of CheA compared to CheW (high CheA occupancy) while *Vibrio cholerae* has a low ratio of CheA compared to CheW (low CheA occupancy) [10].

Chemosensory arrays with high CheA occupancy are expected to form minimal signaling complexes before localization to the cell pole. After localization to the pole minimal signaling complexes oligomerize through CheA-CheA dimerization [6]. Dimerization of CheA acts to link multiple hexagonal rings of alternating CheA and CheW forming arrays with six alternating rings surrounding a CheW only ring (Figure 3A) [6,11]. The regular order and ultrastable structure that results from high CheA occupancy is predicted to be a result of the simplicity of *E. coli* chemotaxis where only 5 MCPs feed into a single chemosensory pathway [2,10].

Species with more complex chemosensory systems tend to have lower CheA occupancy in chemosensory arrays. For example, *Bacillus subtilis* uses 8 membrane bound and 2 cytosolic MCPs to feed a single chemosensory system, and *Vibrio cholerae* uses 38 MCPs to feed its CheII chemosensory system [10,12]. In species that have low CheA occupancy in the baseplate CheW provides cooperativity to the signaling array allowing signals sensed by an MCP that may not be interacting with any CheA to be transduced through multiple CheW proteins before reaching CheA (Figure 4B) [5]. Species with low CheA occupancy arrays also have less structural stability and greater variability of baseplate components that serve functions important for the fine tuning of signal transduction, and the localization of chemosensory arrays (Figure 3B) [10,13]. Proteins involved in baseplate formation contain an array integration and formation (AIF) domain which is homologous in structure to CheW [10]. In addition to CheA and CheW, *V. cholerae* baseplates contain the protein ParP, which functions in recruitment of the

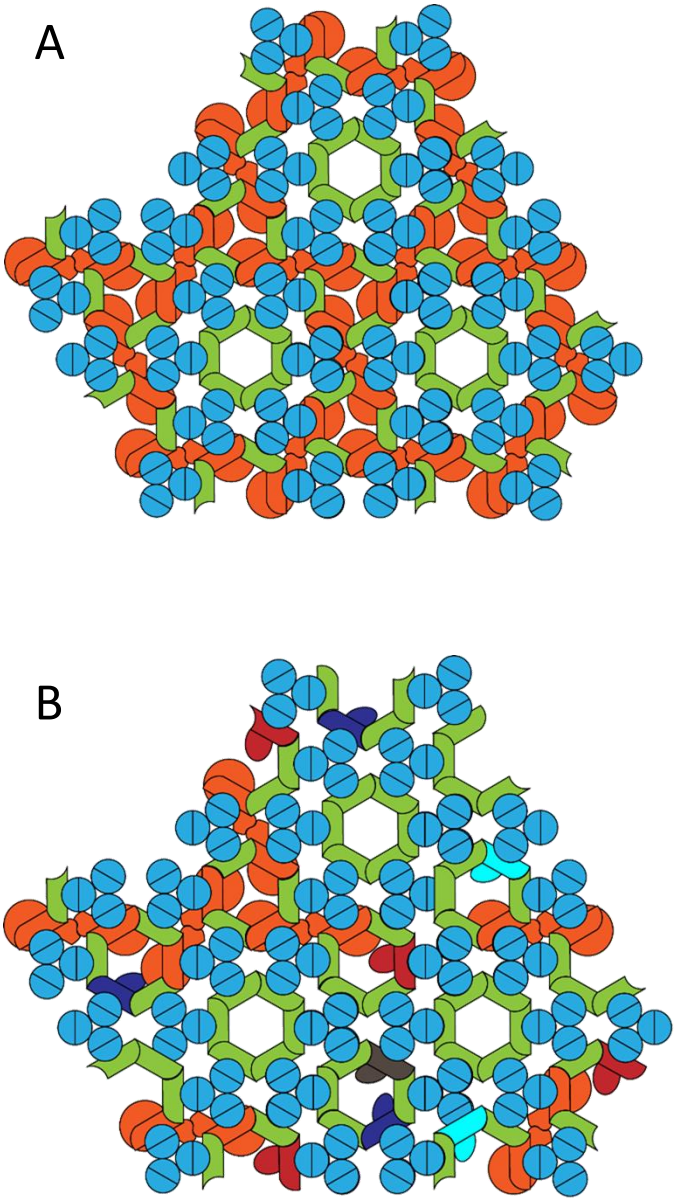

Figure 3 A) Top view of an extended array with high CheA occupancy and no auxiliary components as in *E. coli*. The baseplate is composed of only CheA (orange) and CheW (green). B) Top view of an extended array with low CheA occupancy and auxiliary components as in *V. cholerae.* The baseplate is composed of CheA (orange), CheW (green), CheV1 (navy blue), CheV2 (cyan), CheV4 (grey), and ParP (red). MCP sensory complexes are shown in blue.

chemosensory proteins to the cell pole through interactions between a secondary domain and ParC [13]. *V. cholerae* and *B. subtilis* baseplates also contain the protein CheV, which links a phosphate receiver domain to the baseplate and functions to fine-tune signal transduction in chemosensory systems [10,12,14]. Array formation with low CheA occupancy is expected to occur through a series of individual interactions between MCP trimers of dimers and baseplate proteins after localization to the cell pole [10]. Due to baseplate variability of low CheA occupancy arrays, formation is also expected to be less stable and more dynamic than the ultrastable structure observed in high CheA arrays [10].

Adaptor protein function and structure (CheW)

Formation and localization of chemosensory arrays ultimately relies on interactions between the proteins that make up the array baseplate with each other and with MCPs. The adaptor protein CheW is essential for chemosensory array formation [5,8,15]. CheW is responsible for scaffolding interactions between MCPs, CheA and other baseplate components. CheW also couples CheA to MCP control (Figure 4A) [15,16]. CheW protein has three interaction surfaces (CheW-S1, CheW-S2, CheW-S3). CheW-S1 interacts with surface 2 of the AIF domain of CheA ($CheA_{AIF}$-S2). The interaction of CheW-S1 and $CheA_{AIF}$-S2 is necessary for chemosensory function [17]. CheW-S2 can interact either with surface 1 of $CheA_{AIF}$ ($CheA_{AIF}$-S1) or with another CheW-S1 [5]. The interaction of CheW-S2 enables cooperative function and signal amplification in larger chemosensory arrays (Figure 4B) [5]. CheW-S3 is a hydrophobic cleft that interacts with the cytoplasmic tip of MCPs. Interaction between CheW-S3 and the cytoplasmic tip of MCPs couples conformational changes in the MCP to conformational changes in CheW-S1. Interaction between CheW-S1 and $CheA_{AIF}$-S2 causes the conformational change that induces CheA autophosphorylation [5]. $CheA_{AIF}$ also interacts with the cytoplasmic

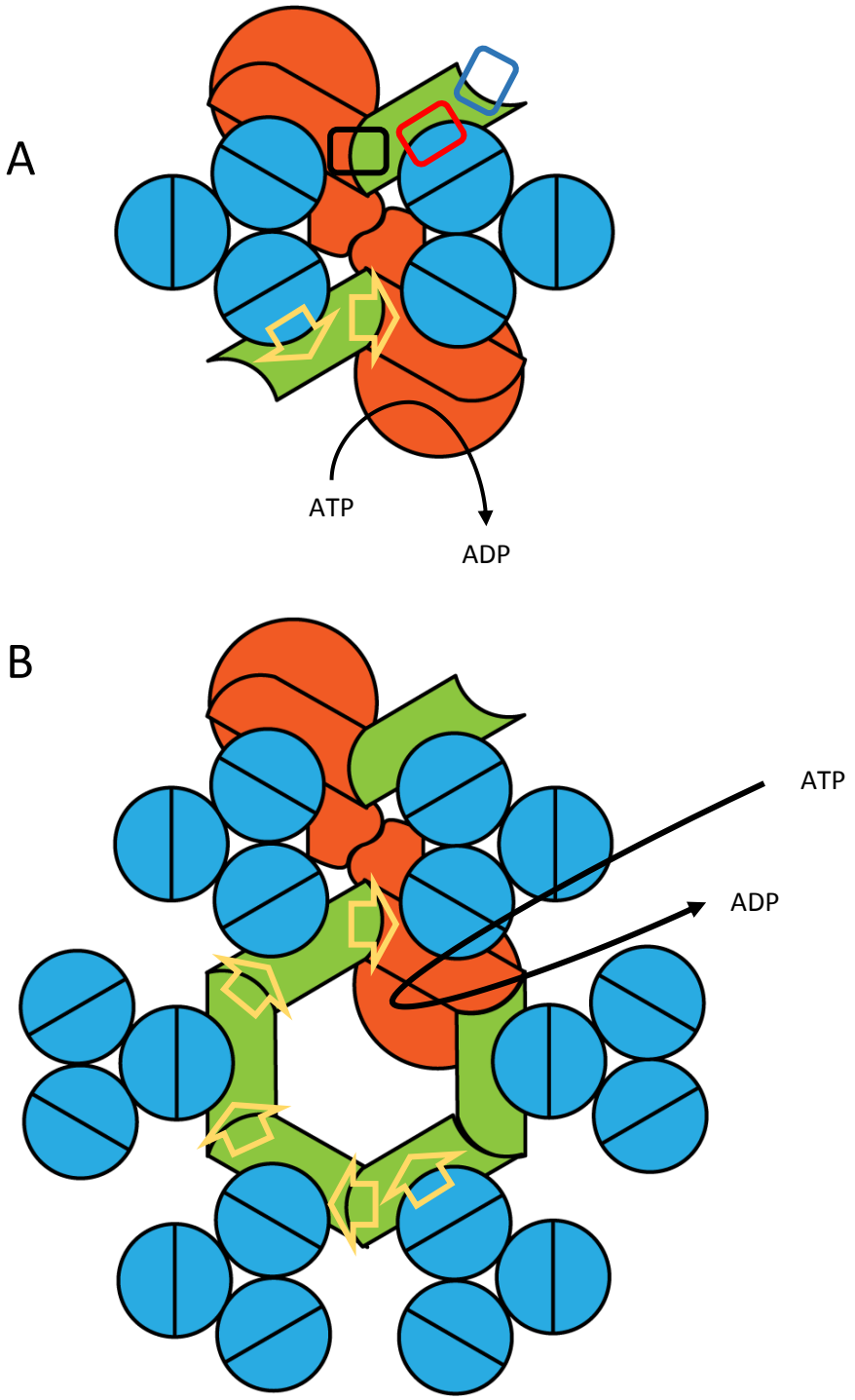

Fig 4. A) Minimal signaling complex showing interaction surfaces of CheW (green) and the direction of conformational change when a signal is sensed. Surface 1 (CheW-S1) is in the black square, surface 2 (CheW-S2) is in the blue square and surface 3 (CheW-S3) is in the red square. When a signal is sensed the conformational change in the MCP is transduced through surface 3 to CheW and through surface 1 to CheA (orange) as shown by yellow arrows. B) Cooperativity of multiple MCP trimers of dimers linked by CheW to a single CheA.

tip of MCPs, however this interaction is not required to induce conformational change in CheA [17]. Fla class chemosensory systems typically encode a single adaptor protein to mediate the interaction between MCPs and CheA [1]. Some Tfp and ACF class chemosensory systems encode multiple adaptor proteins [1]. It is unclear why multiple adaptor proteins are present in these systems. The model bacterium *Pseudomonas aeruginosa* has a complex chemosensory system that includes a Tfp system with two adaptor proteins [1,18,26].

P. aeruginosa chemosensory systems

P. aeruginosa is a Gram negative, rod shaped γ-proteobacterium that is ubiquitous in the environment. It is also an opportunistic pathogen of immunocompromised humans, including those suffering from Cystic Fibrosis, AIDS, and burn injuries. Multi-drug resistant *P. aeruginosa* has recently been classified as a serious threat by the Centers for Disease Control [18,19]. *P. aeruginosa* is also a frequent cause of nosocomial infection and is a pathogen of numerous other eukaryotes [20]. Chronic biofilm infections with *P. aeruginosa* are often recalcitrant to treatment with antibiotics. As a result, *P. aeruginosa* is a model organism for studying pathogenesis, biofilm formation and antibiotic resistance. In order to respond to diverse environments, *P. aeruginosa* encodes a series of proteins that form chemotaxis-like chemosensory systems that facilitate adaptive cellular responses [21].

P. aeruginosa has 4 complete chemosensory systems and one partial chemosensory system encoded in discrete gene clusters. It has 26 predicted MCPs, some of which are encoded within the four gene clusters. The Che I system, which is a Fla class chemosensory system, controls swimming motility. The Che V system encodes an incomplete set of chemosensory homologs most similar to Che I [22,23]. The Che II system encodes a complete chemosensory

cluster of unknown function that is necessary for optimal chemotactic response [24]. The Wsp system, which is an ACF class system, regulates c-di-GMP production and biofilm formation [25]. The Chp system, a Tfp class system and the focus of this thesis, controls twitching motility and cAMP production [26].

The Chp chemosensory system

The *P. aeruginosa* Chp chemosensory system is encoded by a single gene cluster consisting of ten genes (Figure 5). The Chp system controls type IVa pilus (TFP) mediated twitching motility (TM) and modulates cAMP production by the adenyl-cyclase CyaB (Figure 6) [18,27]. TFP are filamentous appendages localized to the poles of *P. aeruginosa* cells that facilitate surface attachment, twitching motility, DNA uptake, virulence and biofilm formation [20,28]. TFP extend by assembly of hundreds of PilA monomers at the base of each pilus structure. Pilus extension is followed by attachment of the distil tip to a surface and disassembly of the PilA filament from the base. This results in pilus retraction and translocation of the cell over a surface (twitching motility) [28]. cAMP produced by CyaB binds to the CAP/CRP-like virulence factor regulator (Vfr). When cAMP is bound, Vfr acts as a homodimer and binds DNA, promoting the expression of over 200 genes. Among these are genes that encode virulence factors, TFP assembly genes, and the TFP associated motor ATPases PilT, PilB, and PilU [18,29]. Despite the two distinct molecular outputs of the Chp system, the end results of cAMP production and direct modulation of TM are inextricably linked [18].

Although the Chp system controls two distinct outputs, it receives input signals through a single MCP (PilJ) [27,30]. Upon signal reception a conformational change is induced at the

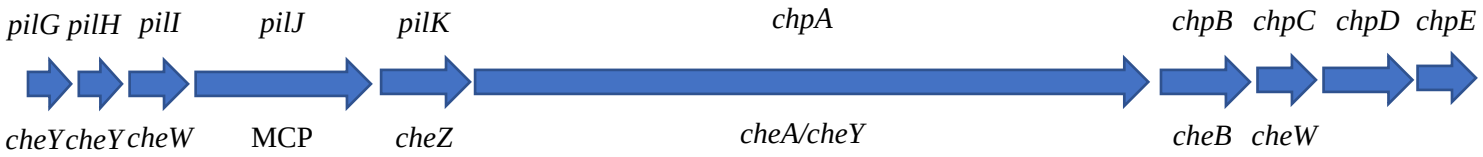

Figure 5 Genetic organization of the *P. aeruginosa* Chp chemosensory system. *P. aeruginosa* gene names are listed above. *E. coli* homologs are listed below.

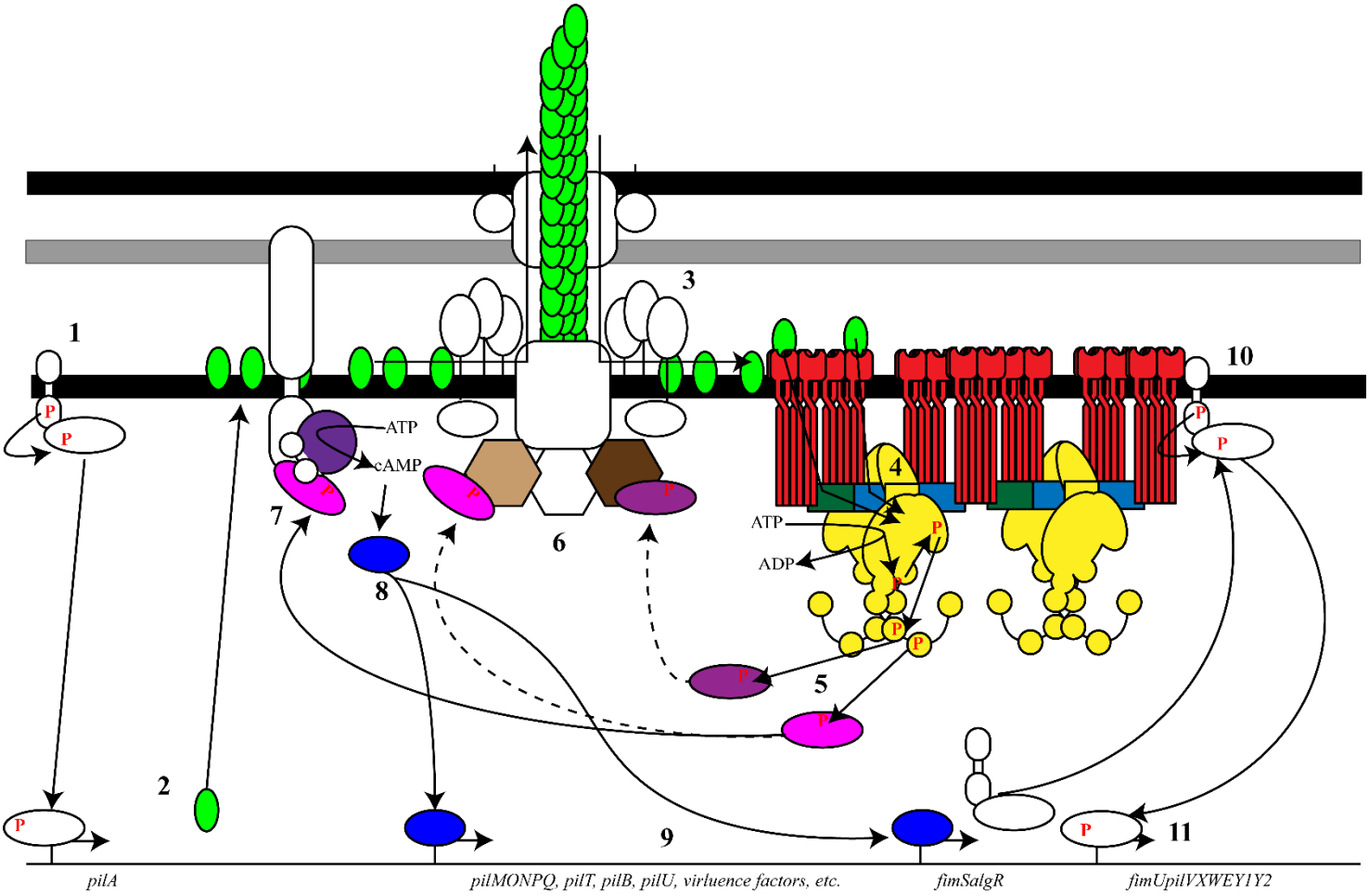

Figure 6 The Chp system and Type IV Pilus. 1) Expression of *pilA* is controlled by the PilRS two component system. 2) PilA (bright green) localizes to the cell poles in the periplasmic membrane. 3) PilA monomers are oligomerized to extend pili, modulated by PilB (tan). PilA monomers are retracted by PilT (brown). Retracted PilA interacts with the periplasmic domain of PilJ (red). 4) Signal is transduced from PilJ to ChpA (yellow) by the adaptor proteins PilI (light blue) or ChpC (dark green) causing phosphorylation of ChpA. 5) ChpA phosphorylates either PilG (pink) or PilH (purple). 6) PilG and PilH may interact with PilB and PilT to modulate extension and retraction. 7) PilG forms a complex with FimL, FimV and CyaB (indigo) to modulate production of cAMP from ATP. 8) cAMP binds to Vfr (royal blue) 9) Vfr induces expression of pilus assembly, alignment and motor genes, virulence factors and the two-component system *fimSalgR*. 10) FimS interacts with PilJ and phosphorylates AlgR. 11) AlgR induces expression of the minor pilin operon.

cytoplasmic tip of PilJ. This conformational change is transduced from PilJ to the histidine kinase (ChpA) [29]. ChpA contains six predicted histidine phosphotransfer domains (Hpt 1-6), a serine phosphotransfer domain (Spt), and a threonine phosphotransfer domain (Tpt), a CheY like receiver domain, a dimerization domain, and an ATPase domain [31]. Only Hpt 2-6 have been demonstrated to be active [31]. Once a conformational change is transduced the ChpA dimer acts in trans to autophosphorylate Hpt 4, 5 or 6 [31]. The phosphate group is then reversibly transferred to the receiver domain in cis before being transferred reversibly to Hpt 2 or 3 or irreversibly to water [31]. Hpt 2 and Hpt 3 then transfer phosphate groups to the receiver domains of the CheY like response regulator proteins PilG and PilH respectively [20]. Phosphorylation of PilH is preferred over PilG allowing PilH to act as a phosphate sink [28]. Phosphorylated PilG (PilG-P) and Phosphorylated PilH (PilH-P) are suggested to function antagonistically to modulate twitching motility by acting on the TFP associated ATPases PilB and PilT respectively, via an unknown mechanism [28]. Modulation of PilB causes pilus extension, while modulation of PilT results in pilus retraction [28]. PilG also modulates the adenyl-cyclase, CyaB, producing cAMP [20]. ChpA also phosphorylates ChpB, a methylesterase predicted to remove methyl groups from PilJ. Together with the methyltransferase PilK, ChpB is responsible for adaptation of Chp signal transduction [18,26].

The interaction between MCPs and a histidine kinase is essential for signal transduction in chemosensory systems. As discussed above, in many chemosensory systems this interaction is mediated by a single adaptor protein, CheW [15,32]. The Chp chemosensory system, like other Tfp class chemosensory systems in γ-proteobacteria, differs from this paradigm and encodes two CheW-like adaptor proteins; PilI and ChpC [26].

How PilI and ChpC effect signal transduction and array formation in the Chp system is not fully understood. Understanding the roles of PilI and ChpC has important implications for understanding chemosensory systems with multiple adaptor proteins as well as implications for understanding *P. aeruginosa* lifestyle decisions and virulence. Elucidating the intricacies of this system will contribute fundamental knowledge regarding complex chemosensory systems and could offer potential avenues for treatment of *P. aeruginosa* infections. This study was conducted to better understand how PilI and ChpC effect downstream targets of Chp signaling, and to determine what role each adaptor protein plays in formation of signaling arrays. We produced a model for Chp chemosensory array formation and signaling based on the data presented in this thesis.

Materials and Methods

Bacterial strains, plasmids and growth conditions

P. aeruginosa PAO1 Iglewski strain was the wild type strain used in this study. *P. aeruginosa* and *E. coli* strains were grown in Lysogeny Broth (LB) at 37°C with aeration in liquid or on 1.5% agar plates unless otherwise indicated. Strains used in this study are listed in Table 1. Experimental DHM1 strains are listed in Table S1. Plasmids used in this study are listed in Table 2. Primers used in this study are listed in Table 3. Antibiotics were used at the following concentrations for *P. aeruginosa*: gentamycin 50 µg/ml; tetracycline 75 µg/ml. Antibiotics were used at the following concentrations for *E. coli*: ampicillin 100 µg/ml; kanamycin 50 µg/ml; gentamycin 10 µg/ml; tetracycline 10 µg/ml.

Table 1: Strains used in this study

Strain	Description	Source
E. coli strains		
DH5αMCR	Cloning strain; *fhuA2 Δ(argF-lacZ) U169 phoA glnV44 Φ80 Δ(lacZ)M15 gyrA96 recA1 relA1 endA1 thi-1 hsdR17*	New England BioLabs
DHM1	Reporter strain for Bacterial Adenylate Cyclase Two-Hybrid Assay; *F-, cya-854, recA1, endA1, gyrA96 (Nal r), thi1, hsdR17, spoT1, rfbD1, glnV44(AS)*	[33]
DHM1 (pKT25-zip pUT18C-zip)	Positive control for Bacterial adenylate cyclase two-hybrid assay	[33]
S17-1	Donor strain for conjugal mating*; TpR SmR recA thi pro hsdR- M+ RP4 2-Tc::Mu-Km::Tn7 λpir*	D. Saffarini
P. aeruginosa strains		
PAO1	wild type (Iglewski Strain)	C. Harwood
PAO1::*lac*P1-*lacZ*	Chromosomal *lacP1* promoter reporter in PAO1 wild type	[33]
Δ*pilI*::*lac*P1-*lacZ*	In frame deletion of *pilI* (PA0410) with 9 amino acids remaining in PAO1::*lac*P1-*lacZ* reporter strain.	This study
Δ*pilI*Δ*pilT*::*lac*P1-*lacZ*	In frame deletion of *pilT* (PA0395) introduced into Δ*pilI*::*lac*P1-*lacZ* strain.	This Study
Δ*chpC*::*lac*P1-*lacZ*	In frame deletion of *chpC* (PA0415) with 9 amino acids remaining in PAO1::*lac*P1-*lacZ* reporter strain.	[35]
Δ*chpC*Δ*pilT*::*lac*P1-*lacZ*	In frame deletion of *pilT* (PA0395) introduced into Δ*chpC*::*lac*P1-*lacZ* strain.	This Study
Δ*cyaB*::*lac*P1-*lacZ*	In frame deletion of *cyaB* (PA3217) with 9 amino acids remaining in PAO1::*lac*P1-*lacZ* reporter strain.	[34]
Δ*cyaB*Δ*pilT*::*lac*P1-*lacZ*	In frame deletion of *pilT* (PA0395) introduced into Δ*cyaB*::*lac*P1-*lacZ* strain.	This study
Δ*pilT*::*lac*P1-*lacZ*	In frame deletion of *pilT* (PA0395) in PAO1::*lac*P1-*lacZ* reporter strain.	[34]
Δ*pilA*::*lac*P1-*lacZ*	In frame deletion of *pilT* (PA0395) in PAO1::*lac*P1-*lacZ* reporter strain.	[34]

Construction of PAO1 deletion strains

In-frame deletions of *pilA, cyaB, pilI, chpC, and pilT* were generated using overlap extension PCR, using primers listed in Table 3. PCR products of the resulting deletion allele were ligated into pEX18Tc and transformed into *E. coli* S17-1 by electroporation. Plasmids were transferred to *P. aeruginosa* by conjugation. *P. aeruginosa* was grown at 42°C without aeration for 30 hours in LB. *E. coli* S17-1 was grown at 37°C overnight in LB with tetracycline (10 µg/ml). 900 µl of *E. coli* S17-1 was centrifuged at 5510 x *g* for 2.5 minutes and washed once with fresh LB. 300 µl of *P. aeruginosa* was added, inverted to mix, and centrifuged at 5510 x *g* for 2.5 minutes. Cells were resuspended in 100 µl of fresh LB and incubated on filter paper on LB agar overnight at 37°C. After incubation cells were removed from the Whatman filter by vortexing in 1 ml LB. The cell suspension was diluted and plated on LB with tetracycline (75 µg/ml) and chloramphenicol (5 µg/ml) for pEX18Tc plasmids. Merodiploids were patched onto LB agar with tetracycline (75 µg/ml) and incubated overnight at 30°C. To allow for the second homologous recombination event, liquid cultures of *P. aeruginosa* merodiploids were grown overnight in LB without antibiotics. Overnight cultures were subcultured to an optical density (OD_{600}) of 0.2 and incubated for 5 hours at 37°C with aeration prior to dilution and plating on LB with 10% sucrose for *sacB* mediated selection. Second recombinants were screened for deletion using PCR. *ΔpilA, ΔcyaB,* and *ΔpilT* strains were produced by Dr. Vibhuti Jansari. *ΔchpC* strain was produced by Swati Sharma. *ΔpilI* strain was produced by Dr. Sonia Bardy.

Construction of *pilI, chpC,* and $cyaB_{R412H}$ expression vectors.

PCR amplified *pilI*, *chpC* and $cyaB_{R412H}$ were ligated into pSB109 (*pilI* and *chpC*) or pJN105 ($cyaB_{R412H}$) and transformed into chemically competent *E. coli* DH5α cells. Constructs were confirmed by sequencing. Purified pSB109 and pJN105 based plasmids were transformed

into *P. aeruginosa* by electroporation. Dr. Vibhuti Jansari constructed pSB109:*pilI* and pJN105:$cyaB_{R412H}$ and Swati Sharma constructed pSB109:*chpC.*.

Electroporation of *P. aeruginosa* PAO1 and *E. coli* S17-1

P. aeruginosa and *E. coli* S17-1 were grown overnight at 37ºC with aeration. 4 ml of culture was centrifuged at 5510 x *g* for 2.5 minutes and washed twice with 10% glycerol. Cells were resuspended in 400 µl of 10% glycerol. 50 µl aliquots were incubated on ice with 200 ng of plasmid DNA and electroporated at 1600 V on an Eppendorf Electroporator 2510 using a 2-mm electroporation cuvette. Cells were suspended in 1 ml of SOC and incubated at 37°C with aeration for 2 hr. Transformants were plated on appropriate antibiotics and incubated at 37°C overnight for pSB109 and pJN105 plasmids and 30°C for 36-48 hours for pEX18Tc plasmids.

Heat shock transformation of *E. coli* DH5α

Chemically competent *E. coli* DH5α cells were incubated on ice with β-mercaptoethanol for 10 minutes, followed by addition of ~200 ng of plasmid and incubation on ice for 30 minutes. Cells were heat shocked at 42ºC for 30 seconds then resuspended in 1 ml of SOC (0.5% yeast extract, 2% tryptone, 10 mM NaCl, 2.5 mM KCl, 10 mM $MgCl_2$ 10 mM $MgSO_4$, 20 mM glucose) and incubated at 37°C with aeration for 1 hour. Cells were plated on LB gentamycin (10 µg/ml) and incubated at 37°C overnight (pSB109 or pJN105) or LB tetracycline (10 µg/ml) and incubated at 30°C for 36-48 hours for pEX18Tc plasmids.

Construction of bacterial two-hybrid expression vectors

PCR amplified *pilI, pilJ,* truncated *chpA,* and *chpC* were purified using Monarch PCR Cleanup Kit before digestion with appropriate restriction endonucleases and ligation into pKT25, pKNT25, pUT18 or pUT18C (BACTH vectors). All BACTH vectors were purified from liquid

Table 2: Plasmids used in this study

Plasmid	Description	Source or reference
pEX18Tc	Gene replacement suicide vector, Tet^R	[36]
pEX18Tc:Δ*chpC*	pEX18Tc based plasmid for deletion of *chpC*	[35]
pEX18Tc:Δ*pilI*	pEX18Tc based plasmid for deletion of *pilI*	This Study
pEX18Tc:Δ*pilT*	pEX18Tc based plasmid for deletion of *pilT*	[27]
pJN105	Expression Vector; Gm^R	[37]
pJN105:$cyaB_{R412H}$	Constitutively active adenyl cyclase *cyaB* cloned into pJN105 at EcoRI and XbaI sites	[27]
pSB109	Arabinose inducible expression vector, Gm^R	[38]
pSB109:*chpC*	*chpC* cloned into pSB109 at EcoRI and SmaI sites	[35]
pSB109:*pilI*	*pilI* cloned into pSB109 at EcoRI and HindIII sites	[35]
pUT18	Bacterial adenylate cyclase two hybrid vector, Amp^R	[33]
pUT18:$chpA_{AA1668-2349}$	*chpA* amino acids 1668-2349 fused in frame at the N-terminus of T18 fragment of the pUT18 plasmid at the XbaI and XmaI sites.	This Study
pUT18:*chpC*	*chpC* fused in frame at the N-terminus of T18 fragment of the pUT18 plasmid at the PstI and EcoRI sites	[35]
pUT18:*pilI*	*pilI* fused in frame at the N-terminus of the T18 fragment of the pUT18 plasmid at the PstI and EcoRI sites	[35]
pUT18:*pilJ*	*pilJ* fused in frame at the N-terminus of the T18 fragment of the pUT18 plasmid at the BamHI and EcoRI sites	[35]
pUT18C	Bacterial adenylate cyclase two hybrid vector, Amp^R	[33]
pUT18C:$chpA_{AA1668-2349}$	*chpA* amino acids 1668-2349 fused in frame at the C-terminus of T18 fragment of the pUT18C plasmid at the XbaI and XmaI sites.	This Study
pUT18C:*chpC*	*chpC* fused in frame at the C-terminus of T18 fragment of the pUT18C plasmid at the PstI and BamHI sites	This Study

pUT18C:*pilI*	*pilI* fused in frame at the C-terminus of T18 fragment of the pUT18C plasmid at the PstI and BamHI sites	This Study
pUT18C:*pilJ*	*pilJ* fused in frame at the C-terminus of the T18 fragment of the pUT18C plasmid at the BamHI and EcoRI sites	This Study
pKNT25	Bacterial adenylate cyclase two hybrid vector, Kan^R	[33]
pKNT25:$chpA_{AA1668-2349}$	*chpA* amino acids 1668-2349 fused in frame at the N-terminus of T25 fragment of the pKNT25 plasmid at the XbaI and XmaI sites	This Study
pKNT25:*chpC*	*chpC* fused in frame at the N-terminus of T25 fragment of the pKNT25 plasmid at the PstI and EcoRI sites	[35]
pKNT25:*pilI*	*pilI* fused in frame at the N-terminus of T25 fragment of the pKNT25 plasmid at the PstI and EcoRI sites	[35]
pKNT25:*pilJ*	*pilJ* fused in frame at the N-terminus of T25 fragment of the pKNT25 plasmid at the BamHI and EcoRI sites	[35]
pKT25	Bacterial adenylate cyclase two hybrid vector, Kan^R	[33]
pKT25:$chpA_{AA1668-2349}$	*chpA* amino acids 1668-2349 fused in frame at the C-terminus of T25 fragment of the pKT25 plasmid at the XbaI and XmaI sites	This Study
pKT25:*chpC*	*chpC* fused in frame at the C-terminus of T25 fragment of the pKT25 plasmid at PstI and BamHI sites	This Study
pKT25:*pilI*	*pilI* fused in frame at the C-terminus of T25 fragment of the pKT25 plasmid at PstI and BamHI sites	This Study
pKT25:*pilJ*	*pilJ* fused in frame at the C-terminus of T25 fragment of pKT25 at BamHI and EcoRI sites	This Study

culture using IBI plasmid mini-prep kit. Concentrations of recovered DNA after restriction digestion were measured on Thermo Scientific NanoDrop 2000C Spectrophotometer and combined in appropriate concentrations for ligation. Ligations were incubated at 16°C overnight before transformation into chemically competent *E. coli* DH5α cells. Transformed cells were selected on LB ampicillin (100 µg/ml) (pUT18 and pUT18C plasmids) or LB kanamycin (50 µg/ml) (pKT25 and pKNT25 plasmids).

Co-transformation of *E. coli* DHM1

E. coli DHM1 was grown overnight at 37°C with aeration. 4 ml of *E. coli* DHM1 overnight culture was centrifuged at 5510 x *g* for 2.5 minutes and washed twice with ice cold 10% glycerol before resuspension in 400 µl of ice cold 10% glycerol. 50 µl aliquots were incubated with 100 ng of each plasmid to be transformed for 30 minutes on ice before electroporation. Cell and DNA suspension were electroporated at 1600V on an Eppendorf Electroporator 2510 using a 2 mm electroporation cuvette. Electroporated cells were resuspended in SOC media and recovered for 2 hours at 37°C with aeration before selection on LB agar containing ampicillin (100 µg/ml) and kanamycin (50 µg/ml). Transformed colonies were isolated on LB with ampicillin and kanamycin before freezing and use in experimental assays. Experimental and control DHM1 strains are listed in Table S1.

Protein-protein interaction assays

Bacterial two-hybrid blue/white screening

DHM1 strains were grown overnight in LB with ampicillin (100 µg/ml) and kanamycin (50 µg/ml) at 30°C with aeration. Overnight cultures were diluted to an OD_{600} of 0.1 and 5 µl of culture was spotted on Blue/White Screening plates (ampicillin 100 µg/ml, kanamycin 50 µg/ml,

Table 3: Primers used in this study

	Primer	Sequence (5'-3')[a]
In-frame deletions	*ΔchpC*_UPFor	TGCCGGAATTCGCAGCGCCACGTGTTGCA
	*ΔchpC*_UPRev	GCTCAGATCAGGCCGGCGTCGGCCTGGTTC ATGTTTCG
	*ΔchpC*_DNFor	CGAAACATGAACCAGGCCGACGCCGGCCT GATCTGAGC
	*ΔchpC*_DNRev	ACAAAGCTTGGAAGCCGCCGGTCAAACCG
	*ΔcyaB*_UPFor	AGGTACCCTTCCGCGATGATCCGCTGG
	*ΔcyaB*_UPRev	GCGCTGGAGAGGATCCCTG
	*ΔcyaB*_DNFor	GCGACCTCTCCTAGGGACGTTCGTCGAACG CCGCCGGCA
	*ΔcyaB*_DNRev	ACTGCAGGTCGTCACCAGCCTGCTGG
	*ΔpilA*_UPFor	CGCGAATTCCGTCCTGCGGTTTGCG
	*ΔpilA*_UPRev	CAAGCCACCTTCGATCACCGCATCTCTCCG TTGATTATG
	*ΔpilA*_DNFor	CATAATCAACGGAGAGATTCGGTGATCGA AGGTGGCTTG
	*ΔpilA*_DNRev	GTCCTGCAGCGGCGGCGACCTTACC
	*ΔpilI*_UPFor	CAGGAATTCGGCTCGCGATTGGGTCGC
	*ΔpilI*_UPRev	TACGGCGACGTCGAGGAAGTCCGACAGGC GGGGCCTG
	*ΔpilI*_DNFor	CAGGCCCCGCATGTCGGACTTCCTCGACGT CGCCGTA
	*ΔpilI*_DNRev	CAGAAGCTTGATGTTGTTCGCCGCTTC
	*ΔpilT*_UPFor	TGGATCCTTGCCGGCGCCGATGAACG
	*ΔpilT*_UPRev	GCGGCGGATCGGCGCCGCCAGGAGGGACT CCCCAATTACAAGCAAG
	*ΔpilT*_DNFor	TGCTTGTAATTGGGGAGTCCCTCCTGGCGC CGATCCGCCGC
	*ΔpilT*_DNRev	GAAGCTTGACAGGTCCATCCACACCTG
Expression	*chpC*-For	CATGCGAATTCATGAACCAGGCCGTGATC
	chpC-Rev	GTATCCCGGGTCAGATCAGGCCGGCGTC
	pilI-For	GTACAGAATTCATGTCGGACGTTCAGACC
	pilI-Rev	CGCGCAAGCTTTTATACGGCGACGTCGAG
	cyaB-For	AGGAATTCATGAAGCCTACCCTCCCCGAC
	cyaB-Rev	ATTCTAGATTAGAGGATGACCTTGTCGCG
	$cyaB_{R412H}$-For	CAGGTGGTGGACTCGCACCGCGACCTCGG CGCC
	$cyaB_{R412H}$-Rev	GGCGCCGAGGTCGCGGTGCGAGTCCACCA CCTG
Bacterial Two-Hybrid	*pilI*_FR-pKT25	GTACTGCAGGGATGTCGGACGTTCAGACC CCCTTC
	*pilI*_FR-KNT-UT-C	GTTCTGCAGGATGTCGGACGTTCAGACCCC CTTC

	*pilI*_RV-KT-UTC	CGGGGGATCCTCTTATACGGCGACGTCGAGGAA
	*pilI*_RV-KNT-UT	CAGGGATCCTCTACGGCGACGTCGAGGAAGCC
	*chpC*_FR-pKT25	GATGCTGCAGGGATGAACCAGGCCGTGATCGAGC
	*chpC*_FR-KNT-UT-C	GAAGCCTGCAGGATGAACCAGGCCGTGATCGAGC
	*chpC*_RV-KT-UTC	CAAGGGATCCTCTCAGATCAGGCCGGCGTCGGC
	*chpC*_RV-KNT-UT	CAGGGATCCTCGATCAGGCCGGCGTCGGCGAG
	*pilJ*_FR	GTCGGATCCCATGAAGAAAATCAACGCAG
	*pilJ*_RV-pKT25	CATTGAATTCTTCAGGCCTGCTCCACGCC
	*pilJ*_RV-KNT-UT/C	GTTAGAATTCGAGGCCTGCTCCACGCCCTC
	*chpA*_FR	GTAACTCTAGACGACGAGAGCGAGATCCT
	*chpA*_RV	GAATACCCGGGGCCGCTGCTGCTCGCTTTC

[a]Restriction enzyme sites are underlined

X-gal 40 µg/ml, and 0.5 mM IPTG). Plates were incubated at 30°C overnight and photographed to document coloration.

Bacterial two-hybrid beta-galactosidase assay

DHM1 strains were grown overnight in LB with ampicillin (100 µg/ml) and kanamycin (50 µg/ml) at 30°C with aeration. Overnight cultures were subcultured to an OD_{600} of 0.1 in LB with ampicillin, kanamycin, and 0.5 mM IPTG to induce expression of fusion proteins. Cultures were grown to mid log phases (OD_{600} 0.4-0.9) at 30°C. 200 µl of culture were suspended in 300 µl of Z-Buffer (6 mM Na_2HPO_4 * 7 H_2O, 40 mM NaH_2PO_4 * H_2O, 10 mM KCl, 1 mM $MgSO_4$ * 7 H_2O, 50 mM β-mercaptoethanol). Cells were lysed using chloroform and 0.1% SDS and incubated at 30°C for 5 minutes. Reactions were started using Z-Buffer with ONPG (4 mg/ml) and stopped through the addition of 1 M Na_2CO_3 after the sample turned yellow. Cell debris was removed by centrifugation at 16873 x *g* for 3 minutes. The OD_{420} of the supernatant was measured and miller units were calculated using the following equation $MU = \frac{OD_{420}}{OD_{600} vt}$ where v represents the volume of culture used in ml and t represents the reaction time in minutes. The assay was performed on three biological samples on three separate days, with each sample assayed with three technical replicates.

Twitching motility assay

Isolated *P. aeruginosa* colonies were stab inoculated into LB plates (1% agar). Plates were incubated at 37°C for 40 hours. Afterwards the agar was removed from the plates and the diameter of the twitching zones was measured.

Beta-galactosidase assay for *P. aeruginosa*

Relative levels of intracellular cAMP were determined using *P. aeruginosa* strains containing the *lac*P1-*lacZ* reporter construct integrated into the genome [17]. Strains were streaked for lawn growth and incubated overnight at 37°C. Cells were scraped from the plate and resuspended in LB broth. OD_{600} was measured and cultures were diluted to an OD_{600} 0.4-0.8. 100 µl of cells were added to 400 µl of Z-Buffer. For strains containing pJN105:$cyaB_{R412H}$, 50 µl of cells were added to 450 µl of Z-Buffer. Beta-galactosidase assays were performed as described above (See: BATCH Beta-Galactosidase Assay)

Western blot analyses

To determine the levels of whole cell PilA expression, strains were streaked for lawn growth and incubated overnight at 37°C. Cells were scraped from the plate and re-suspended in 0.15 M NaCl + 0.2% formaldehyde, and cultures were normalized to 0.6 (OD_{600}). SDS-PAGE loading dye was added and whole cell lysates were prepared by incubation at 95^{o}C for 10 minutes. Protein samples were separated by 15% SDS-PAGE and transferred to a polyvinylidene difluoride (PVDF) membrane. Membranes were probed with anti-PilA (1:10,000) followed by goat anti-rabbit conjugated to peroxidase (1:100,000). Blots were analyzed using Thermo Scientific SuperSignal^{TM} West Femto Maximum Sensitivity Substrate chemiluminescent kit and a Fotodyne Luminary System. Three biological replicates were prepared and quantified using ImageJ software.

Analysis of surface piliation

Strains were streaked for lawn growth and incubated overnight at 37°C. Cells were scraped from the plate and resuspended in 0.15 M NaCl + 0.2% formaldehyde. OD_{600} was

measured and cultures were normalized to 20 (OD_{600}). Surface proteins, including T4P, were sheared from the bacterial surface by vortexing on setting 9 for 30 minutes. Bacterial cells were removed by centrifugation at 12000 x *g* for 5 minutes. Sheared proteins were precipitated in 100 mM $MgCl_2$ overnight at 4^{o}C and pelleted by centrifugation at 16873 x *g* for 25 minutes. Sheared proteins were resuspended in 50 µl PBS and SDS-PAGE loading buffer. PilA monomers were resolved on 15% SDS-PAGE and stained with Coomassie Brilliant Blue (G-250) 4% perchloric acid and photographed on a Fotodyne Luminary System [39]. Three biological replicates were prepared and quantified using ImageJ software.

Statistical analysis

Data were analyzed using a pairwise T-test with multiple variances, and one or two tails as appropriate. The Holm-Bonferroni method was used to correct for multiple pairwise comparisons.

Results

The CheW-like adaptors PilI and ChpC interact with each other

The Bacterial Adenylate Cyclase Two-Hybrid (BACTH) system was used to determine the interaction partners of each adaptor protein of the Chp system. This BACTH system works by reconstituting the active site of the adenylate cyclase CyaA from *Bordetella pertussis* [33]. The active site is divided among two protein fragments; T25 and T18. Genes of interest were cloned into each of four vectors encoding either the T25 or T18 fragment fused in frame. Co-expression of T18 and T25 fusion proteins in *E. coli* DHM1 allowed us to assay for protein interactions. If the two proteins of interest interact, the T25 and T18 fragments are brought into proximity and the active site of *B. pertussis* CyaA is reconstituted. This results in cAMP

production, which binds to CAP/CRP. The cAMP-CAP/CRP complex binds to the *lac* promoter and activates transcription of *lacZ* ultimately resulting in β-galactosidase activity. High β-galactosidase activity, and blue colonies, resulting from cleavage of the colorimetric lactose analog X-Gal, are associated with interaction between the proteins of interest. Low β-galactosidase activity and white colonies are correlated with an absence of interaction between the proteins of interest. Previous preliminary data showed that PilI and ChpC interact with each other using the BACTH system in the PilI-T25/ChpC-T18 and ChpC-T25/PilI-T18 configurations [35]. This interaction was assayed in the remaining six other possible configurations of the BACTH system for PilI and ChpC, all of which resulted in high β-galactosidase activity, and blue colonies on in the colorimetric assay (Figures 7A and B, S1).

PilI and ChpC do not self-interact

PilI and ChpC share only 14.5% sequence identity, and 36% sequence similarity. Most of this similarity occurs at residues expected to be involved with interactions with other proteins containing CheW-like AIF domains. PilI and ChpC also share homology with other proteins containing AIF domains that can integrate into chemosensory arrays such as CheVs. Further, PilI and ChpC interact with each other, leading to our expectation that they would also interact with themselves. However, preliminary data showed this interaction does not occur using the BACTH system. Preliminary work only tested one of the four possible combinations for homodimerization [35]. Since it is possible that interactions may occur in only certain combinations of BACTH vectors due to the relative positions of the T25 and T18 fragments, we chose to test all possible combinations. Similar results were seen for all combinations testing either PilI/PilI or ChpC/ChpC interactions: low β-galactosidase activity similar to empty vector negative controls and white colonies on blue/white plates (Figures 7A and B, S1).

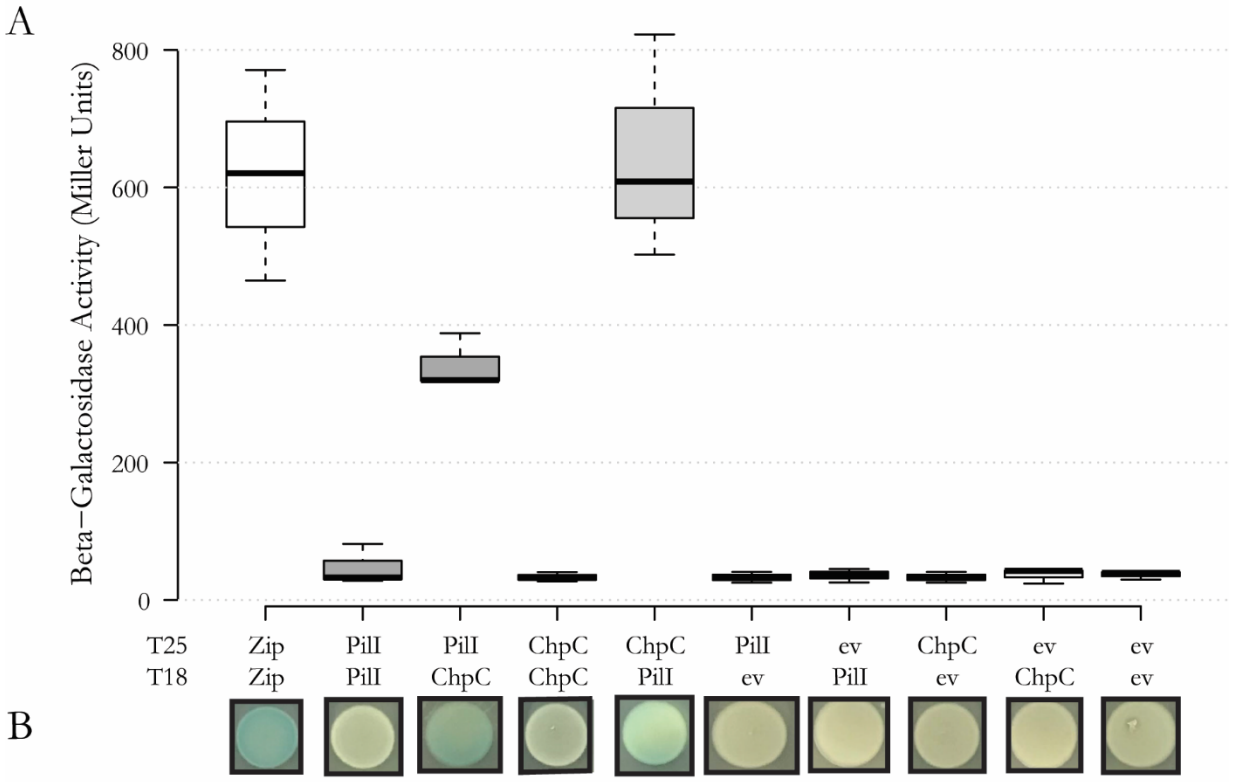
A
Beta−Galactosidase Activity (Miller Units)
800
600
400
200
0
T25 Zip PilI PilI ChpC ChpC PilI ev ChpC ev ev
T18 Zip PilI ChpC ChpC PilI ev PilI ev ChpC ev
B

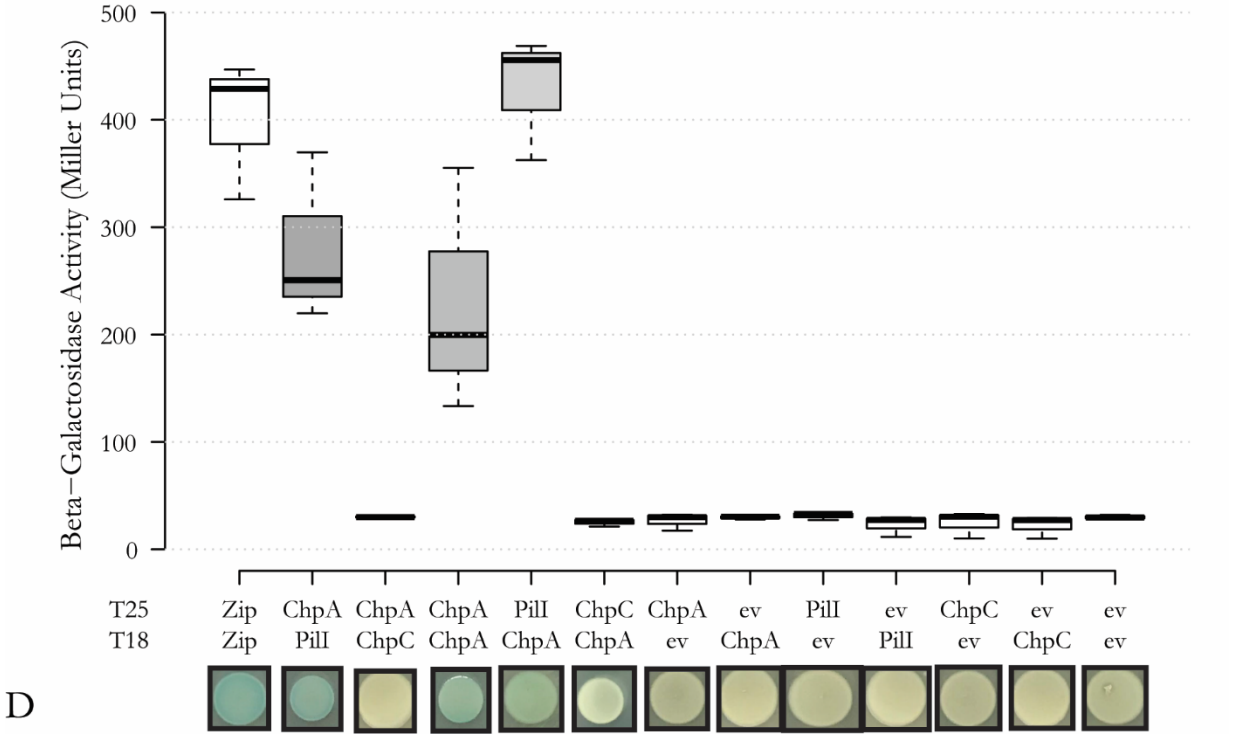
C
Beta−Galactosidase Activity (Miller Units)
500
400
300
200
100
0
T25 Zip ChpA ChpA ChpA PilI ChpC ChpA ev PilI ev ChpC ev ev
T18 Zip PilI ChpC ChpA ChpA ChpA ev ChpA ev PilI ev ChpC ev
D

Figure 7 Bacterial Two Hybrid interaction assays for ChpA, ChpC, and PilI. Each protein of interest was fused to the amino terminal of T25 and the carboxy terminal of T18. 'ev' indicates empty vector. A) β-galactosidase assay showing PilI/ChpC interactions. PilI-T25/T18-ChpC and ChpC-T25/T18-PilI had high β-galactosidase activity compared to empty vector controls, and more consistent with the T25-Zip/T18-Zip positive control, indicating a positive interaction. PilI-T25/T18-PilI and ChpC-T25/T18-ChpC had low β-galactosidase activity consistent with empty vector controls indicating no interaction. B) Blue/White screening showed interaction between PilI and ChpC (Blue) in both PilI/ChpC strains, and no interaction in PilI/PilI or ChpC/ChpC strains (White). C) β-galactosidase assay showing interactions with ChpA. PilI-T25/T18-ChpA and ChpA-T25/T18-PilI had high β-galactosidase activity compared to empty vector controls, and more consistent with the T25-Zip/T18-Zip positive control, indicating a positive interaction. ChpA-T25/T18-ChpA had high β-galactosidase activity compared to empty vector controls, and more consistent with the T25-Zip/T18-Zip positive control, indicating a positive interaction. ChpC-T25/T18-ChpA and ChpA-T25/T18-ChpC had low β-galactosidase activity consistent with empty vector controls indicating no interaction. D) Blue/White screening showed interaction between PilI and ChpA (Blue) in both PilI/ChpA strains, dimerization of ChpA (Blue) and no interaction in either ChpC/ChpA strain (White). For box plots in A and C: center lines show the medians; box limits indicate the 25th and 75th percentiles as determined by R software; whiskers extend 1.5 times the interquartile range from the 25th and 75th percentiles. n = 3 sample points. Each data point is an average of 3 technical replicates.

PilI is the only adaptor to interact with the histidine kinase ChpA.

Because both PilI and ChpC failed to show self-interaction but interact with each other, it became clear that to determine if PilI and ChpC have different roles in the Chp system we needed to look at interactions beyond the adaptors themselves. To explore this, the other predicted constituents of the Chp chemosensory arrays (ChpA and PilJ) were cloned into each of the four BACTH vectors and transformed into experimental DHM1 strains with PilI and ChpC respectively.

The histidine kinase ChpA is a particularly large and complex protein that contains 8 predicted phosphotransfer domains, an ATPase domain, a dimerization domain and a receiver domain. Because of this, we choose to clone the portion of the gene that contained the components necessary for chemosensory function based on homology to the *E. coli* histidine kinase CheA into each BACTH vector to investigate interactions with the histidine kinase ChpA. Truncated ChpA was used in a previous study to determine the activity of phosphotransfer sites of ChpA [31]. This was used as the basis for the ChpA truncation used in this study and corresponded to amino acids 1668-2349 of ChpA which contains one phosphotransfer domain, an ATPase domain, AIF domain and a dimerization domain which corresponds to the globular CheA core. This measure was also taken in order to minimize any spatial hindrance that may occur with such a large protein. Interaction between the histidine kinase and an adaptor is necessary for chemosensory signaling [5,17]. In *E. coli* this interaction occurs only between CheA and CheW, whereas in *P. aeruginosa* it is possible this interaction could occur between ChpA and PilI or ChpA and ChpC.

In the qualitative assay we found that PilI interacts with ChpA by the presence of blue colonies (Figure 7D). This was confirmed by quantitative β-galactosidase assay where all possible combinations of PilI/ChpA produced high β-galactosidase activity correlating with interaction between the two proteins (Figures 7C and S1).

When we tested ChpC/ChpA, we found that experimental DHM1 strains formed white colonies indicative of no interaction between ChpC and ChpA (Figure 7D). To test this quantitatively β-galactosidase assays were performed on all possible combinations of ChpC/ChpA interactions possible in the BACTH system. All combinations of ChpC/ChpA produced low β-galactosidase activity similar to the empty vector negative controls and correlating with no interaction between ChpA and ChpC (Figure 7C and S1).

Together the results for interactions between PilI, ChpC and ChpA suggest that PilI is the primary adaptor protein of the Chp system while ChpC is an auxiliary adaptor.

Interactions with the MCP PilJ

After investigating interactions between PilI and ChpC with ChpA we also wanted to determine the interactions between each adaptor protein and the MCP PilJ. PilJ is necessary for signal transduction through the Chp system, is the only MCP predicted to interact with the Chp system and is co-transcribed with the rest of the Chp system components [27, 30, 40]. However, it has recently been suggested that ChpC integrates another MCP into the Chp chemosensory array [26,41].

Blue/white screening of the PilI/PilJ or ChpC/PilJ DHM1 strains resulted in only white colonies. This trend carried over to quantitative β-galactosidase assays, with all PilI/PilJ and ChpC/PilJ strains having low β-galactosidase activity similar to the empty vector negative

controls (Figure S2). Because PilJ acts as a trimer of dimers, we produced PilJ/PilJ interaction strains to ascertain whether the T18 and T25 fusions were interfering with predicted interactions. We found that all PilJ/PilJ interaction strains produced blue colonies on blue/white plates and showed high β-galactosidase activity (Figure S2). The BACTH system has also been used to show interactions between PilJ and PilA [42]. Therefore, we sought other explanations for why we did not see interactions between PilI/PilJ or ChpC/PilJ.

Based on the similarity of PilI and ChpC to CheW in *E. coli*, the similarity of PilJ to other MCPs, the known architecture of chemosensory arrays, and the colocalization of PilI and PilJ seen previously, we expect that PilI/PilJ, and/or ChpC/PilJ interactions occur in vivo [7]. Both the amino terminal and carboxy terminal fusions of T25 or T18 to PilJ localize the T25 and T18 fragments near the inner membrane. This is sufficient to bring the fragments into close proximity in PilJ/PilJ strains (Figure S3) and PilJ/N-terminal fused PilA strains [42]. In contrast, the tips of PilJ trimers of dimers, where ChpC and PilI would interact, extend approximately more than 28 nm into the cytoplasm [43, 44]. Interactions between MCPs and adaptor proteins have been shown using the BACTH method. In *Helicobacter pylori* TlpA and TlpB interact with CheV1, and TlpA might interact with CheW [15]. The TlpA/CheW interaction was deemed inconclusive, while the TlpA/CheV1 and TlpB/CheV1 interactions were weaker than any interactions shown between two baseplate proteins such as CheV1/CheW [15]. Beyond this, TlpA is from the 28H heptad class and contains a much shorter cytoplasmic domain compared to the 40H PilJ. TlpB is from 40H heptad class, but only interacts with CheV1. Here, the CheY domain of CheV1 may help to bridge the gap to the termini of TlpB. In contrast we expect that when PilJ/PilI or PilJ/ChpC was tested the distance was too great to allow the T25 and T18 fragments to come into each other's proximity to reconstitute the CyaA active site (Figure S3).

From the BACTH data we began to develop a model for chemosensory array formation based on the interactions that occur within the baseplate between PilI, ChpC, and ChpA. In order to refine the model for Chp chemosensory array formation and evaluate the role of the adaptor proteins in Chp chemosensory array formation we produced markerless deletions of *pilI* or *chpC* and assessed the phenotypes of downstream outputs of Chp signaling pathways.

PilI is required for Chp signal transduction

First, in *ΔpilI* we assessed intracellular levels of cAMP bound to Vfr resulting from the modulation of CyaB, and twitching motility resulting from the modulation of PilB and PilT. *ΔpilI* had significantly lowered levels of intracellular cAMP (p=0.013) (~7% of WT). This reduction in cAMP was comparable to the *ΔcyaB* negative control for cAMP production (p=0.181) (~11% of WT) (Figure 8A). *ΔpilI* shows significantly decreased twitching motility ($p=1.14e^{-14}$) (~13% of WT) (Figure 8B). This is similar to the *ΔpilA* negative control that lacks the primary pilin subunit (p=0.346) (~13% of WT).

Next we assessed the surface and whole cell levels of PilA. *ΔpilI* showed significant reductions in both whole cell and surface levels of PilA (Figure 8C and D). In both cases PilA levels were comparable to *ΔcyaB.* This was expected since production of cAMP is necessary for expression of the pilus biogenesis genes [18,45].

It did not escape our notice that reductions in twitching motility, could simply be due to reduced intracellular cAMP resulting in reduced pilus biogenesis rather than reduced actuation of pili. To address this, we transformed *P. aeruginosa* cells with a constitutively active point mutant of CyaB, which we discuss in detail later.

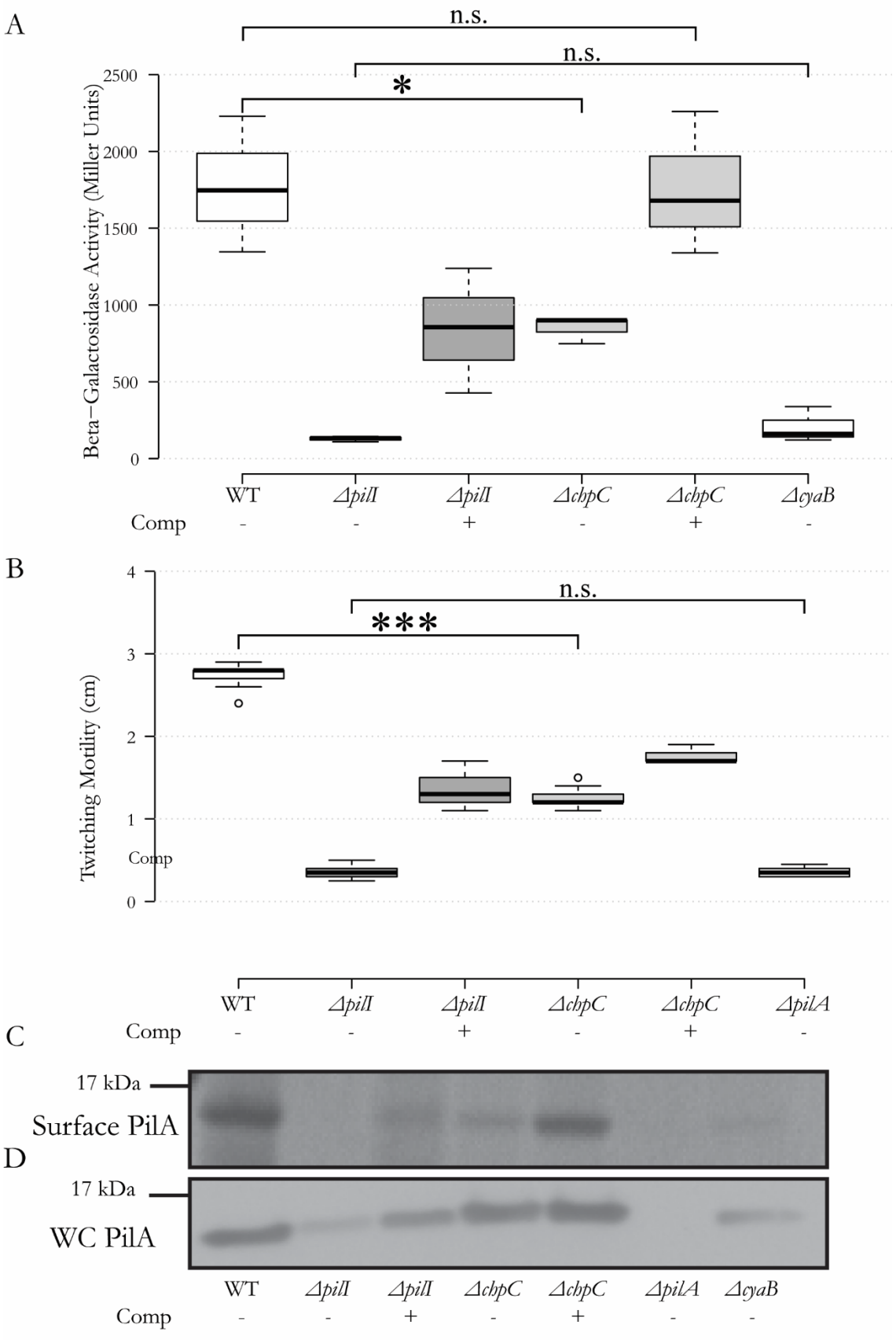
A
n.s.
n.s.
*
Beta−Galactosidase Activity (Miller Units)
2500
2000
1500
1000
500
0
WT
ΔpilI
ΔpilI
ΔchpC
ΔchpC
ΔcyaB
Comp
-
-
+
-
+
-
B
n.s.
***
Twitching Motility (cm)
4
3
2
1
0
Comp
WT
ΔpilI
ΔpilI
ΔchpC
ΔchpC
ΔpilA
Comp
-
-
+
-
+
-
C
17 kDa
Surface PilA
D
17 kDa
WC PilA
WT
ΔpilI
ΔpilI
ΔchpC
ΔchpC
ΔpilA
ΔcyaB
Comp
-
-
+
-
+
-
-

Figure 8 Deletion of *pilI* results in the loss of twitching motility and of intracellular cAMP. Deletion of *chpC* results in a reduction of twitching motility and of intracellular cAMP. A) Indicated strains were assayed for β-galactosidase activity, an indicator of intracellular cAMP bound to Vfr. Center lines show the medians; box limits indicate the 25th and 75th percentiles as determined by R software; whiskers extend 1.5 times the interquartile range from the 25th and 75th percentiles. n = 3 sample points. Each data point is an average of 3 technical replicates. B) Twitching motility of the indicated strains as determined by the diameter of the twitching motility zones. Center lines show the medians; box limits indicate the 25th and 75th percentiles as determined by R software; whiskers extend 1.5 times the interquartile range from the 25th and 75th percentiles, outliers are represented by dots. n = 9 colonies. C) Surface levels of PilA from the indicated strains as determined by SDS-PAGE. D) Whole Cell levels of PilA from the indicated strains as determined by western blotting. In panels A and B asterisks indicate significantly different values (* = $p<0.05$, *** = $p<0.001$) as determined by pairwise T-test and the Holm-Bonferroni correction for multiple comparisons. n.s. indicates values that are not significantly different ($p>0.05$).

When combined these results have helped refine the model presented in this study (Figure 11), suggesting that in *ΔpilI*, Chp chemosensory arrays do not form stable interactions and PilI is necessary and required to transduce conformational change from PilJ to ChpA in order to modulate cAMP production and twitching motility.

Complementation of *pilI* restored cAMP, and twitching motility to ~50% of WT, and only partially restored whole cell and surface PilA levels (Figure 8). This is likely due to one of two possibilities. First, incorrect stoichiometry of PilI:PilJ:ChpA:ChpC resulting from expression of PilI in trans from a non-native promoter could lead to inefficient array formation. Second, when expressed from pSB109:*pilI*, PilI contains a carboxy terminal 6X-His tag. It is possible that the 6X-His tag interferes with interactions necessary for the efficient formation of chemosensory arrays. Complementation of *pilI* with *chpC* in trans did not complement *pilI* for either cAMP levels or twitching motility, further confirming PilI as the primary signaling adaptor, and showing that PilI and ChpC are not redundant (Figure S3).

ChpC is required for Chp signal amplification

In order to evaluate the role of ChpC in Chp chemosensory array formation and to further refine the model presented in this study we produced a markerless deletion of *chpC* and assessed the phenotypes of downstream outputs of Chp signaling pathways. In similar fashion to the *ΔpilI* strain we first assayed intracellular levels of cAMP via a reporter assay to assess modulation of cAMP levels. We also assayed twitching motility to assess modulation of PilB and PilT activity. *ΔchpC* shows reduced levels of intracellular cAMP ($p = 0.031$) (~48% of WT) and reduced twitching motility ($p = 1.30e^{-13}$)(~46% of WT) (Figure 8A and B).

Upon investigating the whole cell and surface levels of PilA we found a reduction of both whole cell PilA and surface PilA in *ΔchpC*. These findings, combined with reduced intracellular cAMP levels and twitching motility allowed refinement of the model presented in figure 11, which suggest that ChpC is an auxiliary adaptor protein that is responsible for signal amplification, through the integration of greater numbers of PilJ receptors and likely contributes to extended array stability.

Complementation of *chpC* restored cAMP and whole cell PilA to WT levels, and partially restored twitching motility and surface piliation (Figure 8A-D). Partial restoration of twitching motility and surface piliation could be due to similar reasons as presented above for *pilI* complementation, however, this is contradicted by the presence of WT levels of cAMP and PilA suggesting that the presence of ChpC has a greater effect on the modulation of CyaB than on twitching. Complementation of *ΔchpC* with *pilI* expressed in trans showed a slight increase in both twitching motility and intracellular cAMP suggesting that overexpression of *pilI* could partially restore signaling, however this effect was found to be insignificant with p values of 0.135 for cAMP and 0.052 for twitching motility (Figure S3).

Excess cAMP restores twitching motility in *ΔchpC*

Since the Chp chemosensory system directly modulates twitching motility [28], but also modulates cAMP production which is necessary for the expression of pilus assembly and motor genes we expressed a constitutively active point mutant of CyaB. $CyaB_{R412H}$ produces cAMP independent of Chp chemosensory signaling and has been used previously to overcome cAMP deficiencies to study pilus function in other Chp system mutants [26]. When $cyaB_{R412H}$ was expressed in *ΔpilI, ΔchpC* or *ΔcyaB* it produced similar levels of cAMP ($p > 0.05$) that were approximately twice the level in WT cells (Figure 9A)

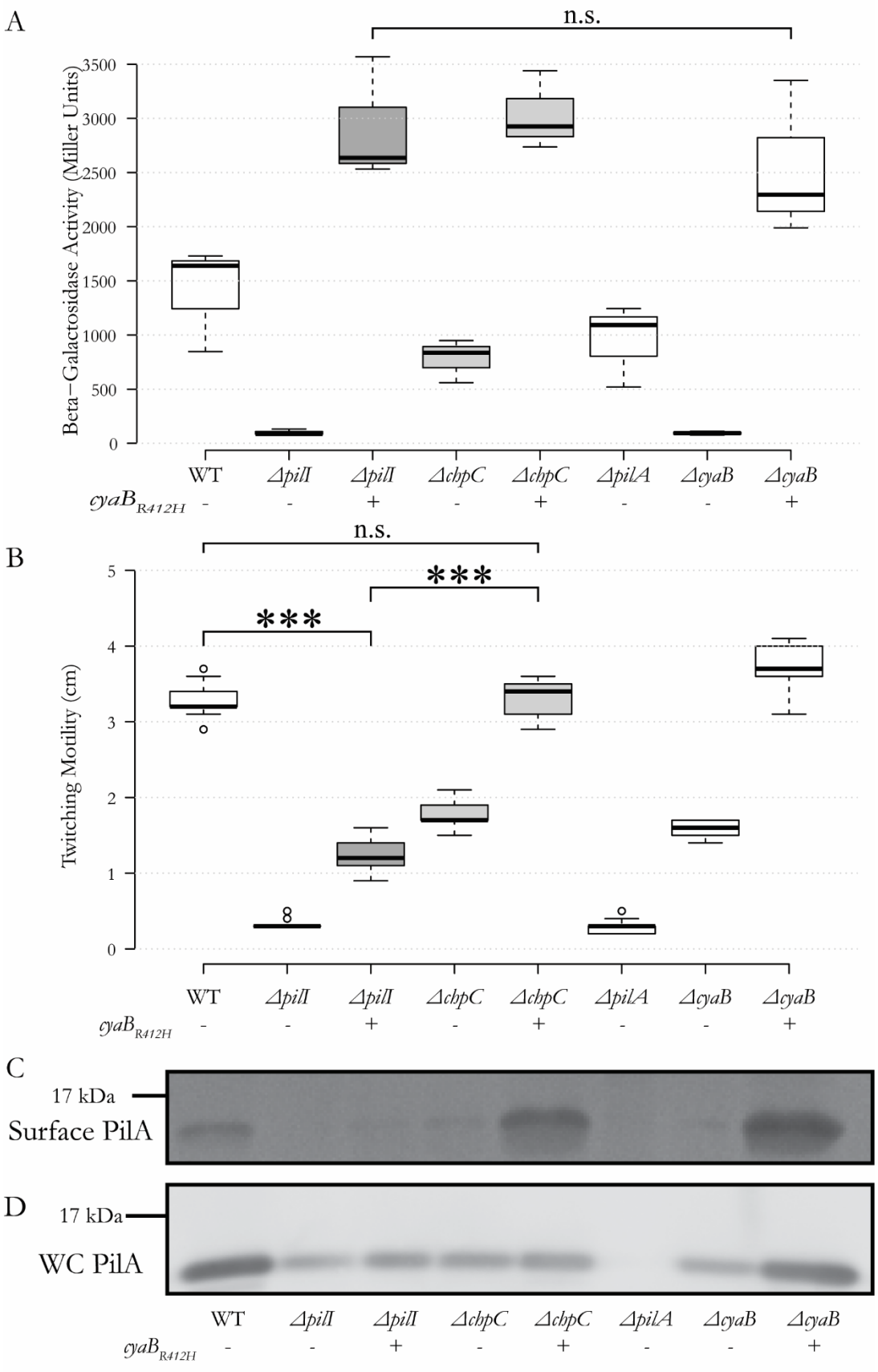
A
n.s.
Beta−Galactosidase Activity (Miller Units)
3500
3000
2500
2000
1500
1000
500
0
WT
ΔpilI
ΔpilI
ΔchpC
ΔchpC
ΔpilA
ΔcyaB
ΔcyaB
cyaB R412H
- - + - + - - +
B
n.s.
***
***
Twitching Motility (cm)
5
4
3
2
1
0
WT
ΔpilI
ΔpilI
ΔchpC
ΔchpC
ΔpilA
ΔcyaB
ΔcyaB
cyaB R412H
- - + - + - - +
C
17 kDa
Surface PilA
D
17 kDa
WC PilA
WT
ΔpilI
ΔpilI
ΔchpC
ΔchpC
ΔpilA
ΔcyaB
ΔcyaB
cyaB R412H
- - + - + - - +

Figure 9 Expression of *cyaB*$_{R412H}$ point mutant provides excess cAMP and restores WT twitching motility in *ΔchpC*. A) Indicated strains were assayed for β-galactosidase activity, an indicator of intracellular cAMP bound to Vfr. Center lines show the medians; box limits indicate the 25th and 75th percentiles as determined by R software; whiskers extend 1.5 times the interquartile range from the 25th and 75th percentiles. n = 3 sample points. Each data point is an average of 3 technical replicates. B) Twitching motility of the indicated strains as determined by the diameter of the twitching motility zones. Center lines show the medians; box limits indicate the 25th and 75th percentiles as determined by R software; whiskers extend 1.5 times the interquartile range from the 25th and 75th percentiles, outliers are represented by dots. n = 9 colonies. C) Surface levels of PilA from the indicated strains as determined by SDS-PAGE. D) Whole cell levels of PilA from the indicated strains as determined by western blotting. In panels A and B asterisks indicate significantly different values (*** = $p<0.001$) as determined by pairwise T-test and the Holm-Bonferroni correction for multiple comparisons. n.s. indicates values that are not significantly different ($p>0.05$).

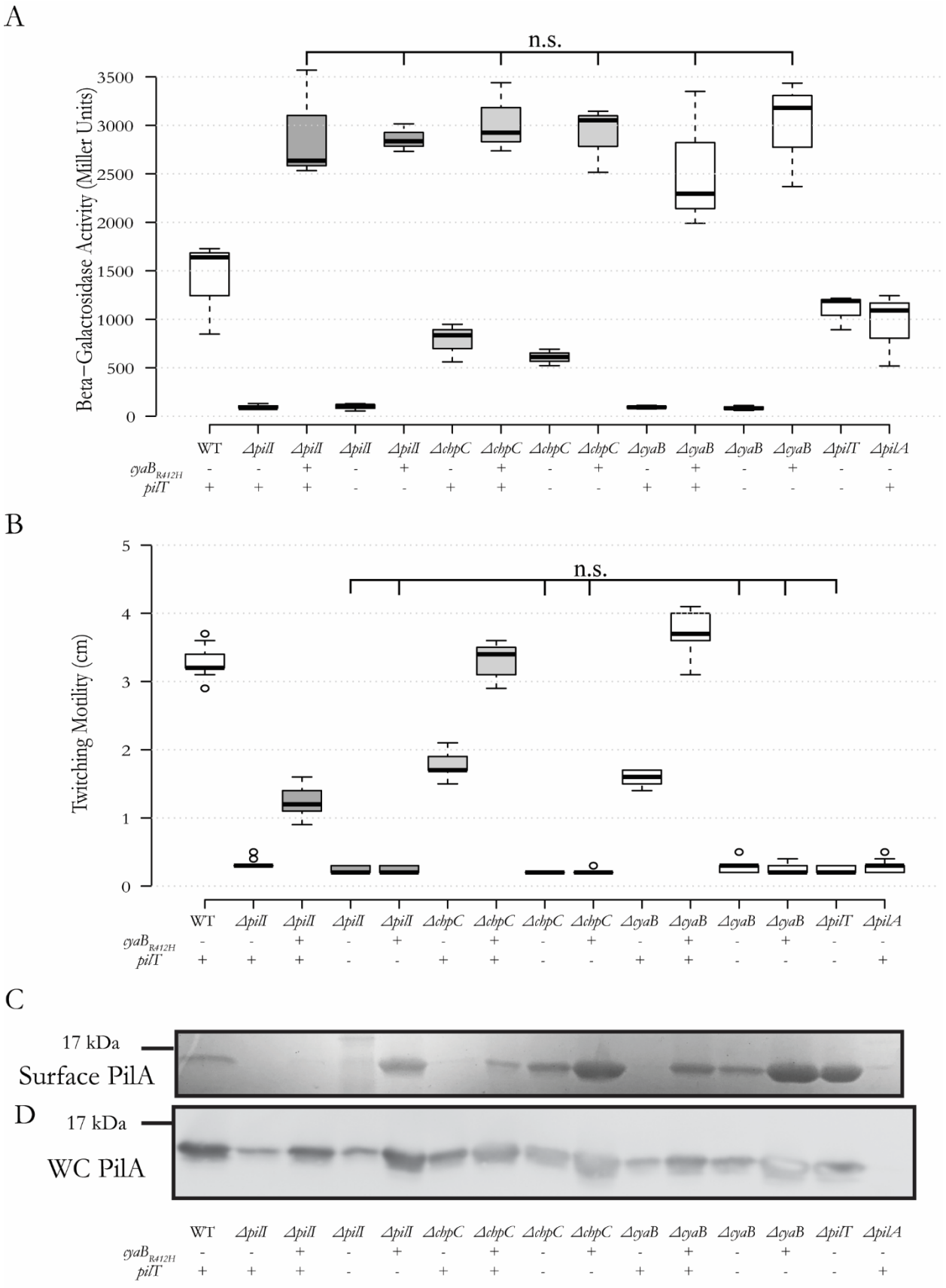
A
n.s.
Beta−Galactosidase Activity (Miller Units)
3500
3000
2500
2000
1500
1000
500
0
WT ΔpilI ΔpilI ΔpilI ΔpilI ΔchpC ΔchpC ΔchpC ΔchpC ΔcyaB ΔcyaB ΔcyaB ΔcyaB ΔpilT ΔpilA
cyaB R412H - - + - + - + - + - + - + - - -
pilT + + + - - + + - - + + - - - +
B
n.s.
Twitching Motility (cm)
5
4
3
2
1
0
WT ΔpilI ΔpilI ΔpilI ΔpilI ΔchpC ΔchpC ΔchpC ΔchpC ΔcyaB ΔcyaB ΔcyaB ΔcyaB ΔpilT ΔpilA
cyaB R412H - - + - + - + - + - + - + - - -
pilT + + + - - + + - - + + - - - +
C
17 kDa
Surface PilA
D
17 kDa
WC PilA
WT ΔpilI ΔpilI ΔpilI ΔpilI ΔchpC ΔchpC ΔchpC ΔchpC ΔcyaB ΔcyaB ΔcyaB ΔcyaB ΔpilT ΔpilA
cyaB R412H - - + - + - + - + - + - + - - -
pilT + + + - - + + - - + + - - - +

Figure 10 Deletion of *pilI* results a loss of pilus extension. Expression of *cyaB*$_{R412H}$ results in elevated cAMP. Deletion of *pilT* results in a loss pilus retraction, and loss of twitching. A) Indicated strains were assayed for β-galactosidase activity, an indicator of intracellular cAMP bound to Vfr. Center lines show the medians; box limits indicate the 25th and 75th percentiles as determined by R software; whiskers extend 1.5 times the interquartile range from the 25th and 75th percentiles. n = 3 sample points. Each data point is an average of 3 technical replicates. B) Twitching motility of the indicated strains as determined by the diameter of the twitching motility zones. Center lines show the medians; box limits indicate the 25th and 75th percentiles as determined by R software; whiskers extend 1.5 times the interquartile range from the 25th and 75th percentiles, outliers are represented by dots. n = 9 colonies. C) Surface levels of PilA from the indicated strains as determined by SDS-PAGE. D) Whole Cell levels of PilA from the indicated strains as determined by western blotting. In panels A and B 'n.s.' indicates values that are not significantly different ($p>0.05$) as determined by pairwise T-test and the Holm-Bonferroni correction for multiple comparisons.

When we expressed *cyaB*$_{R412H}$ we saw increased twitching motility when compared to each respective strain without *cyaB*$_{R412H}$. In *ΔchpC*(*cyaB*$_{R412H}$) and *ΔcyaB*(*cyaB*$_{R412H}$) this resulted in restoration of twitching motility to WT level (p = 0.500) (Figure 9B). In *ΔchpC*(*cyaB*$_{R412H}$) this means that Chp signaling transduced by PilI is sufficient to support twitching motility in the absence of ChpC when excess cAMP is present. This also suggests that a critical level of intracellular cAMP must be reached before twitching motility occurs, and that Chp arrays lacking ChpC may not transduce enough signal to modulate CyaB activity to cause a sufficient increase in cAMP. In *ΔpilI*(*cyaB*$_{R412H}$) this increase does not restore twitching motility to WT levels (p = 3.72e^{-12}). Increased twitching in *ΔpilI*(*cyaB*$_{R412H}$) could be explained by increased cAMP causing an increase in expression of T4P biogenesis and motor function genes and a corresponding increase in whole cell PilA. PilT and PilB, the motor ATPases of T4P retain a small amount of residual activity in the absence of Chp signaling, which could explain the slight increase in twitching motility in *ΔpilI*(*cyaB*$_{R412H}$).

Expression of *cyaB*$_{R412H}$ resulted in increased whole cell PilA when compared to each respective strain without *cyaB*$_{R412H}$. In *ΔchpC*(*cyaB*$_{R412H}$) and *ΔcyaB*(*cyaB*$_{R412H}$) this resulted in dramatically increased surface piliation. In *ΔpilI*(*cyaB*$_{R412H}$) the increase in whole cell PilA resulted in a comparably minute increase in surface piliation, and can be explained as above, by residual PilB activity combined with increased PilA (Figure 9D). This confirms that PilI is the primary adaptor protein and can support pilus function in the absence of ChpC when cAMP is provided separate from Chp signal transduction.

We examined the discrepancy in restoration of twitching motility between *ΔchpC(cyaB*$_{R412H}$*)* and *ΔpilI(cyaB*$_{R412H}$*)* thoroughly to determine whether it was due to a lack of pilus extension or over-retraction as proper pilus function is required for twitching motility. We

made a retraction mutant by deleting the gene encoding the retraction ATPase, *pilT*, in *ΔpilI* and *ΔchpC*, and the appropriate controls. Next we transformed each strain with pJN105:$cyaB_{R412H}$ to restore cAMP production separate from Chp signaling. All strains assayed expressing $cyaB_{R412H}$ displayed increased cAMP as expected ($p > 0.05$) (Figure 10A). All *ΔpilT* strains were null for twitching motility resulting from the inability to retract pili ($p > 0.05$) (Figure 10B). We observed similar trends in whole cell PilA as described above in *ΔpilT* strains where each strain expressing $cyaB_{R412H}$ had increased levels of whole cell PilA compared to each respective strain without $cyaB_{R412H}$ (Figure 10D). Whole cell PilA levels were similar in each *ΔpilT* strain relative to one another and were restored to near WT level (Figure 10D). In *ΔchpCΔpilT*($cyaB_{R412H}$) and *ΔcyaBΔpilT*($cyaB_{R412H}$) this resulted in significant increases in surface piliation to above WT level, but comparable to that of *ΔpilT* (Figure 10C). This confirms functional extension of pili in *ΔchpCΔpilT*($cyaB_{R412H}$) where chemosensory arrays consist of only PilJ:PilI:ChpA. In *ΔpilIΔpilT*($cyaB_{R412H}$) the increase in whole cell PilA resulted in a comparably small increase in surface piliation that can be explained by residual PilB activity, and increased expression of genes necessary for pilus biogenesis resulting from increased cAMP as explained earlier (Figure 10C). This confirms that without PilI present, the Chp system fails to modulate pilus extension.

Model for Chp chemosensory array formation

Based on the conclusions drawn from BACTH and phenotypic data, we constructed and refined a model for Chp chemosensory array formation. Interactions that lead to the formation of the baseplate are essential for chemosensory array formation and provide the framework for regularly interspaced MCP trimers of dimers, so we focused on these interactions to produce the model depicted in Figure 11. It has previously been reported that the interaction between the adaptor protein surface 1 (CheW-S1) and surface 2 of the histidine kinase AIF domain ($CheA_{AIF}$-

S2) is necessary for transduction of conformational change and induction of autophosphorylation (Figure 4) [5,17]. In the Chp chemosensory system this corresponds to surface 1 of PilI (PilI-S1) interacting with surface 2 of the AIF domain of ChpA ($ChpA_{AIF}$-S2). Cooperative function and extended array formation results from the interaction of the adaptor protein surface 2 (CheW-S2) with either surface 1 of the histidine kinase AIF domain ($CheA_{AIF}$-S1) or with CheW-S1 of another CheW molecule (Figure 4) [5,17]. In the Chp chemosensory system this corresponds to surface 2 of PilI (PilI-S2) interacting with surface 1 of the AIF domain of ChpA ($ChpA_{AIF}$-S1) and surface 1 of ChpC (ChpC-S1), since PilI cannot interact with itself (Figure 7A and B). Based on PilI-S2 interacting with $ChpA_{AIF}$-S1 and ChpC-S1, and PilI-S1 interacting with $ChpA_{AIF}$-S2, we took the logical step that PilI-S1 also interacts with ChpC-S2.

Figure 11A models a Chp chemosensory array in WT. We expect that each hexagonal ring consists of three PilI monomers interspaced by a combination of $ChpA_{AIF}$, and ChpC. We predict that a hexagonal ring consisting of a 3:1:2 ratio of PilI:$ChpA_{AIF}$:ChpC would be the most effective at transducing a signal to ChpA, as it integrates signal from five PilJ receptors into a single ChpA, however it is most likely that hexagonal rings consisting of 3:3:0, 3:2:1, 3:1:2 and 3:0:3 ratios of PilI:$ChpA_{AIF}$:ChpC all exist within one array. The interchangeability of each type of hexagonal ring likely lends to a dynamic, sensitive, structurally flexible, but stable array.

Figure 11B depicts a Chp chemosensory array in *ΔpilI.* Because the ChpC adaptor failed to show interaction with ChpA we predict that no stable chemosensory complexes form resulting in loss of Chp signal transduction. This would explain the lack of cAMP production, loss of twitching motility, reduced PilA levels and loss of surface piliation in *ΔpilI* (Figure 8).

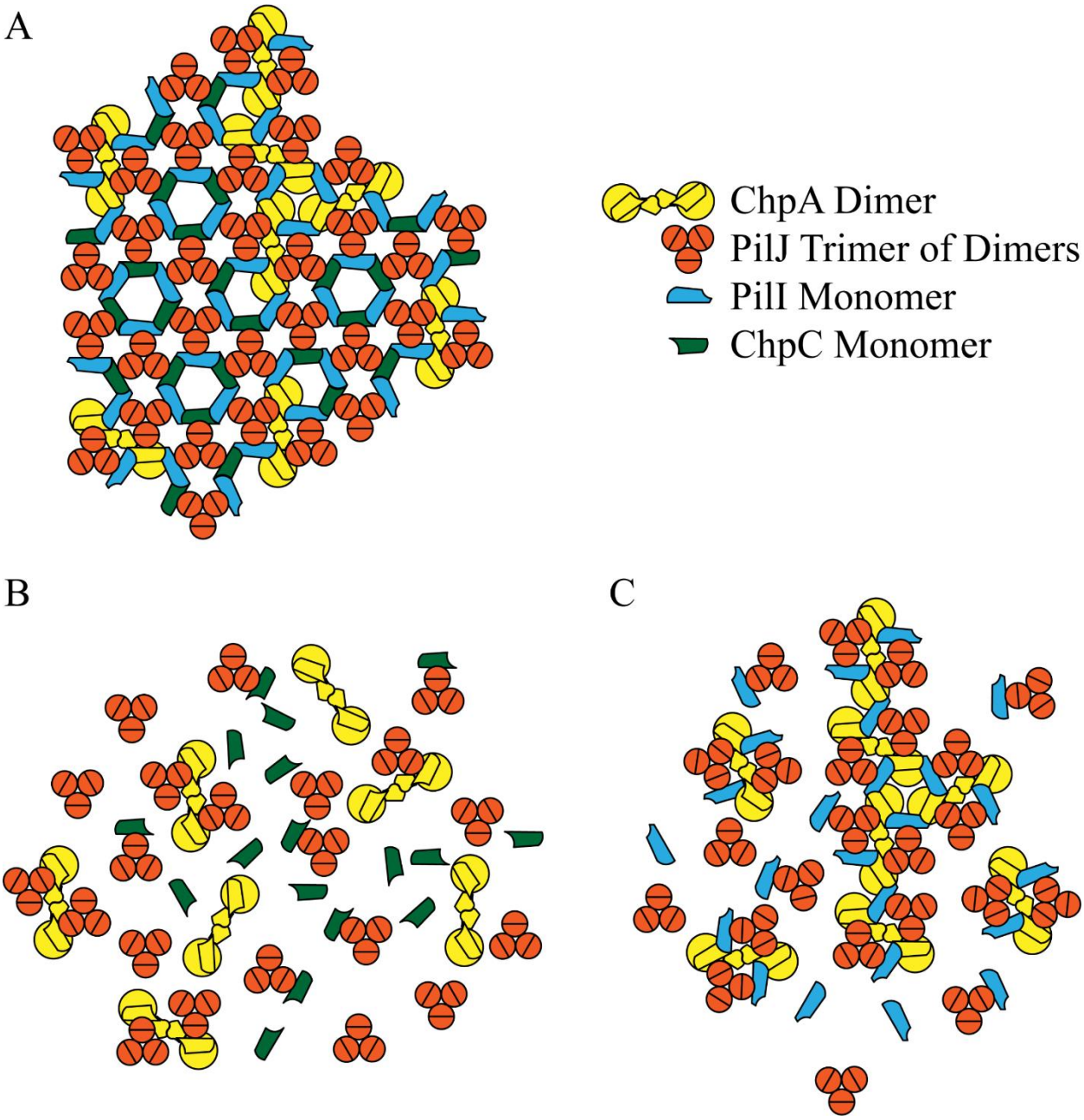

Figure 11 Chp chemosensory array model. ChpA dimers are shown in yellow, PilJ trimers of dimers are shown in orange, PilI is shown in light blue, and ChpC monomers are shown in dark green. A) Modeled Chp chemosensory array in PAO1 WT based on BACTH interaction data. B) Modeled Chp chemosensory array in PAO1 *ΔpilI* strain. C) Modeled Chp chemosensory array in PAO1 *ΔchpC* strain.

Figure 11C depicts a Chp chemosensory array in *ΔchpC*. Because PilI and $ChpA_{AIF}$ interact on both surface 1 and surface 2 we predict that array formation is still possible in *ΔchpC*. the only possible hexagonal ring in these arrays contain a 3:3:0 ratio of PilI:$ChpA_{AIF}$:ChpC meaning only two PilJ receptors can be integrated to each ChpA. These arrays, therefore, are expected to be smaller, less efficient, less sensitive, structurally less flexible and less stable than WT arrays. We predict that this would lead to a reduction in phosphorylated ChpA and therefore reduced cAMP and reduced twitching motility which is consistent with phenotypes observed in *ΔchpC*. The smaller arrays formed in *ΔchpC* are sufficient to modulate twitching motility when cAMP production is separated from Chp signaling. Based on the mechanosensory model, an actively twitching cell would be a high signal environment which could explain why the smaller arrays in *ΔchpC(*$cyaB_{R412H}$*)* are able to support twitching motility when cAMP is produced independently. This is also consistent with reduced twitching in *ΔchpC* being the result of insufficient cAMP causing lowered expression of pilus assembly, alignment and motor genes, resulting in decreased PilA and surface piliation.

Discussion

Adaptor proteins are an essential, but often overlooked, component of chemosensory signaling systems. Mutants lacking adaptor proteins are non-chemotactic, resulting from the inability to form chemosensory arrays, and therefore inability to transduce chemosensory signals [2,6]. While canonical studies have been done in chemosensory systems that contain a single adaptor protein, the presence of multiple adaptors is quite common and distributed amongst at least 12 different phyla and multiple classes of chemosensory systems [1]. The F6 and F10 type systems of the Fla class of flagellar chemosensory systems, ACF class systems, which control alternative cell functions, and Tfp class systems, which control twitching motility, all contain multiple

adaptor proteins. Tfp class systems are found in 6 bacterial phyla, and in the γ-proteobacteria Tfp class systems frequently include a second adaptor protein [1].

One of these, the Chp system of *P. aeruginosa*, also controls two regulatory outputs via a single MCP, PilJ, and histidine kinase, ChpA [27]. Here, our newfound understanding of the roles of two adaptor proteins, PilI and ChpC, in the Chp system shed light on other Tfp class chemosensory systems and other chemosensory systems that contain multiple adaptor proteins.

Twitching is a common form of bacterial motility, and it is assumed that the primary function of Tfp class chemosensory systems is modulation of twitching motility, however, functional Tfp class systems are understudied. Fortunately, a series of recent studies have identified functional Tfp class systems with differing levels of homology to the Chp system in *P. aeruginosa.*

The phytopathogen *Ralstonia solanacaerum* has a Tfp system analogous to the *P. aeruginosa* Chp system that controls twitching motility and is implicated in initial stages of infection in plants [46]. This Tfp system however does not encode a secondary adaptor protein ChpC, the putative methylesterase ChpB or the methyltransferase PilK. The fact that twitching motility is functional in this bacterium is not surprising as PilI can support twitching on its own when cAMP is supplied independently in *P. aeruginosa*. This begs the question of how pilus biogenesis is regulated in *R. solanacaerum.* In another phytopathogen, *Xanthomonas oryzae*, a putative Tfp system has been identified [47]. This Tfp system, like the one identified in *R. solanacaerum*, lacks PilK, ChpB and ChpC. Interestingly, *X. oryzae* uses a separate two component system homologous to PilRS in *P. aeruginosa* to control expression of T4P related genes and to control pilus biogenesis [47].

Given the similarities between the Chp systems of *R. solanacaerum* and *X. oryzae*, as compared to *P. aeruginosa*, we expect that *R. solanacaerum* is unlikely to modulate cAMP production using its Tfp chemosensory system, and T4P assembly and motor genes are likely regulated by a different system. From this, it stands to reason that the additional adaptor found in *P. aeruginosa* is necessary to produce large enough, or sensitive enough, signaling arrays for sufficient signal amplification to regulate alternative outputs, such as cAMP production, in addition to twitching motility.

Oddly, the phytopathogenic bacterium, *Xylella fastidiosa*, also contains a functional Tfp system that controls only twitching motility [48]. The *X. fastidiosa* Tfp system encodes the secondary adaptor protein ChpC, but lacks PilH, PilK, and encodes a degenerate ChpB expected to be non-functional [48]. How exactly this relates to *P. aeruginosa* retaining the multifunctional Chp system with PilH, PilK, ChpB, and ChpC, and other bacteria with the simplified Tfp system is uncertain, but it suggests that chemosensory adaptation is less important in *X. fastidiosa*, which could be the result of its highly specialized niche lifestyle [48].

Curiously, Tfp class systems that encode PilK, ChpB and ChpC are almost exclusively found in γ-proteobacteria [1]. This poses a number of interesting questions that could be answered using *P. aeruginosa*. First, our evidence suggests that the secondary adaptor protein ChpC may be necessary for Tfp class systems to have multiple outputs. It stands to reason that Tfp systems like the Chp system are more sensitive and more adaptive given the presence of a methyltransferase, PilK, and a methylesterase, ChpB. It is possible that the adaptive methylation plays a role in determining which of the Chp systems outputs is regulated. While phenotypes have been observed in *ΔpilK* and *ΔchpB*, adaptive responses of the Chp system are not well studied, because *pilK* complementation has proven particularly recalcitrant [18,26]. As a result,

the trend that *chpC* is typically only present with both *pilK* and *chpB* remains a curiosity and potential avenue for further study.

While Tfp systems with multiple adaptor proteins like the Chp system are nearly exclusive to γ-proteobacteria, the presence of multiple adaptor-like proteins is seen in other chemosensory systems [1]. The auxiliary protein CheV, which consists of a CheW like AIF domain, fused to CheY like REC domain, can transduce signal from an MCP to CheA, as well as attenuate signal by acting as a phosphate sink. From this perspective any system containing one or more CheVs could be considered to have multiple adaptor proteins.

In at least one case, CheV is the only adaptor protein in a functional chemosensory system. *Listeria monocytogenes* is a chemotactic bacterium. Its genome does not encode a CheW protein, but does include the other essential components and CheV, thus suggesting CheV has potential to be a bonafide adaptor protein [1,49].

Whether CheV directly interacts with CheA in the same manner as CheW or requires the presence of CheW in extended chemosensory arrays is not well studied and is likely dependent on the organism. It is expected that some CheV proteins have co-evolved with specific MCPs and function to integrate these MCPs into chemosensory arrays that contain a non-cognate CheW [1], while others may act in a more promiscuous sense within chemosensory arrays by interacting with multiple MCPs, and directly with CheA.

In *Vibrio cholerae* the CheII chemosensory system is known to form highly unstable chemosensory arrays that integrate at least two of the four CheVs present [10]. However, these CheV proteins are present in particularly small quantity when compared with CheW resulting in the likelihood that deletion of any of the specific CheV proteins would have a minute effect on chemotaxis, while deletion of CheW would result in a non-chemotactic strain. Likely, CheV in

this system is not acting as a primary adaptor like PilI in *P. aeruginosa* but is instead acting in an auxiliary role like ChpC.

Helicobacter pylori presents a different case. Its genome encodes one CheW and three CheVs which interact within one chemosensory system [15]. In this case, deletion of CheW results in a non-chemotactic strain, while deletion of CheV1 results in functionally impaired chemotaxis [15,50]. Deletion of CheV2 and CheV3 has no effect on chemotaxis [50]. CheW is acting as the primary adaptor and could be compared to PilI in the Chp system as deletion in either case leads to a loss of motility. CheV1 presents a few different possibilities. It could be acting similarly to ChpC, where it functions as an auxiliary adaptor, causing signal amplification in extended arrays as deletion in either case results in only impaired motility. Alternatively, the loss of CheV1 could result in the subsequent loss of certain MCP integration. The inability to transduce signal from CheV1s cognate MCP(s) would result in impaired chemotaxis, however, this would likely be condition specific. Again, it is likely that CheV still requires the presence of CheW to transduce signal to CheA, similar to our model presented for PilI and ChpC.

The integration of a CheV protein is not the only way for a chemosensory system to integrate multiple adaptors. Chemosensory systems have been described that make use of multiple CheW proteins. For example, in *Agrobacterium tumefaciens* two CheW proteins are integrated into a single chemosensory system [51]. Each CheW functions as a primary adaptor, like PilI in the Chp system, but each function with different efficacies. Only deletion of both $CheW_1$ and $CheW_2$ results in a complete loss of motility. Deletion of $CheW_2$ results in a greater loss than deletion of $CheW_1$ suggesting that each is integrated into chemosensory arrays either in different amounts or with different affinities. The genetic organization of the *A. tumefaciens* chemosensory system is interesting. Rather than being present in a single cluster or operon the

genes are distributed individually amongst the genome [51]. Importantly each CheW is under the control of its own promoter, and the activity of these promoters accounts for differential amounts of each protein, with the $CheW_2$ promoter being stronger than $CheW_1$ [51].

In *Rhodobacter sphaeroides* two CheW proteins were expected to interact with a single chemosensory system [52]. Interestingly the role of each CheW is dependent on growth conditions. $CheW_2$ is required for chemosensory function under all conditions tested, while $CheW_3$ was necessary under photoheterotrophic growth conditions [52]. Whether this is due to expression or integration of each adaptor was not addressed. In this case both $CheW_2$ and $CheW_3$ most likely function as primary adaptors like PilI. What specifically makes $CheW_3$ required only under photoheterotrophic growth conditions, however, is still unknown.

The integration of two CheW proteins into a single chemosensory system is also seen in *Borrelia burgdorferi* [53]. In this case $CheW_1$ and $CheW_3$ were both shown to interact with $CheA_2$ [53]. Arrays were directly visualized using electron cryotomography and they found that deletion of *cheW*$_3$ resulted in complete loss of array formation, while deletion of *cheW*$_1$ resulted in arrays that were significantly smaller than in WT [53]. This result not only confirms that multiple CheW can exist in the same array simultaneously but is also consistent with our model for Chp chemosensory array formation where we predict that deletion of *chpC* would result in smaller arrays and deletion of *pilI* results in a complete loss of array formation. It is interesting to note that both $CheW_1$ and $CheW_3$ interact with $CheA_2$, which is different than our proposed model where only PilI interacts with ChpA.

The suggested inability of ChpC to interact with ChpA could be the result of a structural difference in ChpC-S1 compared to PilI-S1 that makes ChpC unable to interface with $ChpA_{AIF}$-S2. This is similar to how FrzB functions in *Myxococcus xanthus* [54]. The *M. xanthus* Frz

system incorporates two adaptor proteins, FrzA and FrzB. FrzA is the primary adaptor and transduces signal directly from FrzCD to FrzE [54]. FrzB, on the other hand, is structurally divergent from the typical CheW and lacks two β-strands typically seen on surface 1 [54]. Thus, FrzB cannot interface with FrzE. When the two β-strands from FrzA are added to FrzB, the ability to interface with FrzE is conferred [54]. In WT *M. xanthus*, Frz system arrays localize to multiple locations on the nucleoid. Oddly, when *frzB* is deleted, the arrays all coalesce into a single larger array suggesting that FrzB has a somewhat disruptive effect on array formation, rather than a cooperative one as we expect for ChpC.

While the presence of multiple adaptor-like proteins is relatively common, we can see from the systems discussed above that multiple adaptors are used in a variety of manners, all of which share only partial congruence with PilI and ChpC in the Chp chemosensory system. For this reason, we think that our insights into Chp chemosensory function and our model of array formation are particularly interesting.

We found that both PilI and ChpC are required for WT function of the Chp chemosensory system, however, each is required to differing degrees. We found that PilI makes a stronger contribution to Chp signaling than ChpC as evidenced by the null phenotype for intracellular cAMP and twitching motility, reduction in whole cell PilA and lack of surface piliation in *ΔpilI* cells. *ΔchpC* cells on the other hand only have partially depleted levels of intracellular cAMP, show reduced twitching motility, whole cell PilA and surface piliation. From this we concluded the PilI is the primary signaling adaptor and ChpC is an auxiliary adaptor required for signal amplification. Separation of cAMP production from Chp signaling strengthened the position of PilI as the primary adaptor, as seen by the restoration of twitching motility in *ΔchpC(cyaB*$_{R414H}$*)*.

Analysis of the interactomes of PilI and ChpC also showed differential functions. PilI and ChpC interact with each other, suggesting that Chp chemosensory arrays incorporate both adaptors at the same time. PilI and ChpC and do not self-interact, suggesting that arrays incorporating only one of the two adaptors are smaller or less stable. Crucially, it was found that only PilI is able to interact with a truncated ChpA solidifying its role as the primary signaling adaptor, and suggesting PilI is necessary for array formation. It is worth noting that ChpC may interact with a domain or folded conformation not present in the truncated ChpA used in this study. We suspect this is unlikely given the current understanding of CheW/$CheA_{AIF}$ interactions, which were used to design the ChpA truncation used here [31].

From this we developed a model for Chp chemosensory array interactions that lead to array formation. As a starting point, the hexagonal pattern of the baseplate and regular spacing of MCPs within the baseplate is universally conserved among bacteria and archaea [7,8]. Examples of this pattern can be seen in Figures 2, 3 and 11A. Our model suggests that the hexagonal rings of Chp chemosensory arrays are comprised of PilI monomers alternating with either ChpA or ChpC where the ratio of PilI:ChpA:ChpC can range from 3:0:3 to 3:3:0, with a 3:1:2 ratio (low ChpA occupancy) being the most sensitive to signal acquisition, and 3:3:0 ratio (high ChpA occupancy) being the least sensitive (Figure 12).

Since multiple hexagonal rings are held together by ChpA dimers, it makes sense to discuss sensitivity of Chp chemosensory arrays on a per ChpA dimer basis. Two connected rings consisting of a 3:1:2 ratio would integrate the maximum of 10 PilJ sensory complexes into a single ChpA dimer for 10:1 sensitivity ratio. While a 3:1:2 ratio produces the maximum sensitivity ratio, it would not contain any exterior points at which ChpA dimerization interactions could occur. Therefore, arrays consisting entirely of 3:1:2 rings would be dependent on

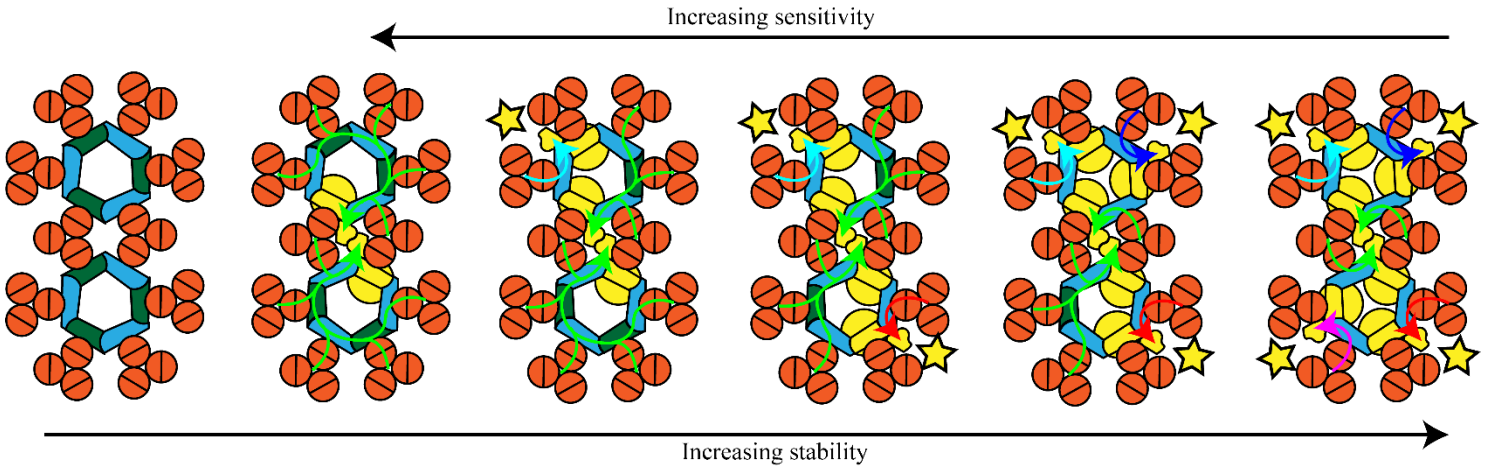

Figure 12 Possible hexagonal ring formations for the Chp chemosensory array. PilJ receptor complexes are represented in orange. PilI is light blue. ChpC is dark green. ChpA is Yellow. Arrows denote which ChpA dimer each PilJ receptor complex would transduce signal to. Different color arrows represent different ChpA dimers. Yellow stars denote points where dimerization of ChpA would allow for extend array formation. As ChpA occupancy increases, dimerization potential and stability increases. As ChpA occupancy decreases, sensitivity increases.

interactions between the baseplate and PilJ to produce extended arrays likely leading to structural instability (Figure 12).

Alternatively, two 3:3:0 rings would integrate 10 PilJ sensory complexes into 5 ChpA dimers resulting in a 2:1 sensitivity ratio. However, a pair of 3:3:0 rings would contain 4 exterior ChpA dimerization points. This could allow for more stable array formation to occur since the extended lattice would be dependent on both baseplate/PilJ interactions and ChpA dimerization interactions (Figure 12).

Two 3:2:1 rings would be the functional intermediate regarding both sensitivity and structural stability with an average sensitivity ratio of 4:1, and 2 external ChpA dimerization points. While all four possible ratios of rings exist within a single Chp chemosensory array, we expect most rings to be either 3:1:2, or 3:2:1 ratios to balance the sensitivity of integrating the largest possible number of PilJ sensory complexes to as few ChpA dimers with the extended lattice stability provided by having multiple ChpA dimers attached to a single ring.

Beyond experimental data obtained from the BACTH system and phenotypic assays, we developed our model based on previous inquiries made into chemosensory array structure. We considered both high and low ChpA occupancy as options for Chp array formation. While both scenarios are possible, we chose to present our model with low ChpA occupancy, for the following reasons. First, low ChpA occupancy allows higher input sensitivity, as discussed above. Second, high ChpA occupancy arrays retain much of their structure in the absence of ChpC. Third, the large physical size of full length ChpA [26,31]. Fourth, arrays with low CheA occupancy tend to integrate auxiliary components such as CheVs [10]. Fifth, low CheA occupancy arrays are more dynamic and able to adapt to environmental changes [10]. Finally, *P.*

aeruginosa contains a Che chemosensory system similar to *V. cholerae* which is known to have low CheA occupancy.

If Chp arrays were to form with high ChpA occupancy, when ChpC is absent the structure of the arrays would remain mostly intact, and we would expect to see little to no difference between levels of cAMP, twitching motility, whole cell PilA and surface piliation in WT when compared to *ΔchpC*. Since we do see a reduction in all the aforementioned phenotypes in *ΔchpC* as compared to WT we concluded that low ChpA occupancy is more likely. Further, a high ChpA occupancy array would contain hexagonal rings consisting of only 3:3:0 or 3:0:3 PilI:ChpA:ChpC. This would mean that the arrays are less sensitive to signal received by PilJ as only two PilJ receptor complexes could be integrated into each ChpA. Since PilI is unable to interact with itself, the formation of 4:2, 5:1, or 6:0 PilI:ChpA rings would not be possible as they are in *V. cholerae* (CheW:CheA) [10]. We again expect to see little to no change in phenotype for *ΔchpC* when compared to WT. Since this is not the case it further supports a low ChpA occupancy array.

ChpA is also an approximately 280 kDa protein, consisting of 2477 amino acids [26]. This is much larger than the typical CheA. Because of this, we expect that fitting three ChpA dimers into close proximity as would be required in a high ChpA occupancy array would result in significant steric hinderance potentially destabilizing the overall structure of the array. Our data also suggests that ChpC is not involved in direct interaction with ChpA and therefore is unable to directly transduce signal. Since ChpC only functions to increase sensitivity and amplify the signal received by PilJ we present ChpC as an auxiliary component of Chp chemosensory arrays, much as CheVs are considered auxiliary components in low CheA occupancy arrays such as those seen in *V. cholerae*, rather than treating PilI and ChpC collectively as a single CheW

[10]. In *V. cholerae* CheVs attenuate signal received by MCP clusters, and in *P. aeruginosa* ChpC is required to amplify signal sensed by PilJ. Since the high CheA occupancy arrays of *E. coli* do not contain any auxiliary baseplate components, this further solidifies the case for low ChpA occupancy in Chp arrays.

Lastly, *P. aeruginosa* encodes a Che chemosensory system with homology to the *V. cholerae* Che system, which is known to be a low CheA occupancy array [10]. Because of this similarity, we expect that *P. aeruginosa* Che system arrays would be of low CheA occupancy and expect this would carry over to the Chp systems arrays. Also, arrays with low CheA occupancy are generally associated with bacteria with more complex and adaptable chemosensory systems. *P. aeruginosa* is highly adaptable and has many complex chemosensory systems of which the Chp system is only a portion leading us to conclude the Chp arrays would have low ChpA occupancy.

Our model for chemosensory array formation is consistent with a mechanosensory model of Chp signal transduction in a broader context as presented by Persat et al. [42]. In this model, surface naïve cells express a low basal level of genes necessary for pilus biogenesis and function. The initial signal sensed by the system is the result of tension in a pilus fiber when the cell encounters a surface, and PilA monomers are retracted into the inner membrane. PilJ transduces signal via either PilI directly, or ChpC and PilI in series, to ChpA causing autophosphorylation. ChpA-P phosphorylates PilG and PilG-P modulates CyaB activity to produce cAMP. cAMP binds to Vfr and induces expression of pilus assembly, alignment and motor genes. Once more pili have been assembled PilG-P and potentially PilH-P modulate twitching motility by an undetermined mechanism that could involve interactions with the motor ATPases PilB and PilT respectively. Our model adds the specificity to how signal is transduced from PilJ to ChpA.

Alternatively, it has been suggested that ChpC may act to integrate another, as yet unidentified, MCP into Chp arrays [41]. In the model proposed by Nolan, et al. ChpC integrates signal from another MCP that binds a small molecule and directly transduces the signal from that MCP to ChpA in a complex consisting of MCP, ChpC, and ChpA [41]. This modulates a twitching response via PilG and PilH interactions with PilB and PilT. Retracted PilA monomers interact with PilJ, which signals ChpA via PilI in a separate complex consisting of PilJ, PilI and ChpA to modulate CyaB via PilG and PilH, resulting in the expression of T4P genes and a continued twitching response [41].

It must be noted that the model presented in Nolan, et al. has not been peer reviewed, and we have some concerns regarding the conclusions they have drawn. Their experiments fail to provide cAMP independent of Chp signaling. In this study we have shown that providing cAMP independent of Chp signaling via $CyaB_{R412H}$ restores twitching in *ΔchpC* and we expect that supplemental cAMP would restore twitching to WT levels in their experiments. We expect the phenotype seen by Nolan, et al. was due to lowered cAMP and therefore lowered expression of genes necessary for T4P biogenesis and therefore twitching motility. Despite these concerns, their model merits further discussion.

Based on the demonstrated reduction in twitching motility, intracellular cAMP, whole cell PilA, and surface piliation in *ΔchpC* we expect that ChpC and PilJ interact. However, the BACTH method proved insufficient to draw conclusions regarding PilJ interactions with ChpC or any other baseplate components, nor would interaction between PilJ and ChpC preclude ChpC from interacting with another MCP. Therefore, we cannot disregard the possibility of a secondary MCP.

Our experiments using the BACTH system do show that ChpC does not interact with a truncated ChpA in any of the possible vector combinations. Therefore, we conclude ChpC is unable to transduce signal directly to ChpA, which suggests that separate chemosensory complexes consisting of MCP/ChpC/ChpA and PilJ/PilI/ChpA do not exist. Also, data obtained using the BACTH system show that PilI and ChpC interact with each other, suggesting Chp signaling complexes incorporate both PilI and ChpC into a single array.

This, however, is not enough to conclusively reject an alternative MCP as ChpC could transduce signal to ChpA via interactions with PilI in extended chemosensory arrays. Only MCPs of the same heptad class are able to integrate into the arrays containing multiple MCPs [44,55]. PilJ is of the 40H heptad class, and the *P. aeruginosa* genome encodes 20 other 40H heptad class MCPS. However, this is not the only requirement necessary to determine which chemosensory system an MCP will localize to. It is possible to computationally assign MCPs to specific chemosensory systems based on not only on heptad class, but also methylation sites, and conserved residues involved in the interaction between the receptor tip and the adaptor protein [30]. Based on computational data combining all of these factors for MCPs in *P. aeruginosa*, only PilJ is assigned to the Chp system, with all other 40H heptad class MCPs assigned to either the CheI system (19) or the Wsp system (1)[30].

Deletion of PilJ causes loss of both cAMP production and twitching motility [27]. Further, deletion of the periplasmic receptor domain of PilJ causes a defect in twitching motility that is restored when cAMP is provided separate of Chp signaling showing that PilJ can modulate twitching motility independently of cAMP production [27]. The model presented by Nolan, et. al suggests that PilJ is only involved in the modulation of cAMP, and therefore only

indirectly involved in modulating twitching motility rather than being directly involved in modulating twitching motility as has been published.

In *Xylella fastidiosa,* a system homologous to the Chp system in *P. aeruginosa* containing the genes for both PilI and ChpC integrates only a single PilJ-like MCP into its chemosensory system, because the *X. fastidiosa* genome encodes only one MCP [48]. Finally, *R. solanacaerum* encodes a Tfp class chemosensory system homologous to the *P. aeruginosa* Chp system but lacking PilK, ChpB and ChpC. This system is necessary for twitching motility in *R. solanacaerum,* where deletion of *chpA* or *pilI* resulted in a loss of motility, and complementation restored motility [46]. This further suggests that ChpC is not required to initiate a twitching response, however any connection to cAMP production has not been studied in *R. solanacaerum.*

In the event that further experiments show that ChpC integrates a second MCP into the Chp system the model presented in this study would require only minor amendment to account for the second MCP. No amendment to how the hexagonal rings of the array baseplate are formed would be required and ChpC would remain an auxiliary component.

In summary, our work has shown that PilI is the primary adaptor in the Chp system, plays a greater role in signal transduction than ChpC, and we suggest PilI is the only adaptor to interface directly with the histidine kinase ChpA. While signal amplification necessary for effective chemosensory function in the Chp system requires both adaptors, twitching motility can be restored in a *ΔchpC* mutant when cAMP is provided independent of Chp signal transduction. Together, we used these results to construct a model for chemosensory array formation in the Chp system consistent with the interactome of each adaptor protein and the phenotypes observed in their absence. Experiments to determine the structure of each adaptor are ongoing and could lead to further insight into how each adaptor interacts with other baseplate components of the

Chp system. Furthermore, studying the effect of *ΔcpdA* is of interest in relation to the Chp system as it allows cAMP build up in the cell. CpdA is a phosphodiesterase but leaves the modulation of CyaB, and therefore production of cAMP, under control of the Chp system. These experiments are also ongoing. Future study into the mechanism by which PilG determines whether it modulates CyaB or PilB are of interest as are experiments to determine how adaptive responses effect Chp signal transduction.

References

1. Wuichet, K., Zhulin, I. B. (2010) Origins and diversification of a complex signal transduction system in prokaryotes. *Sci. Signal, 3*(2010). doi:10.1126/scisignal.2000724
2. Wadhams, G., Armitage, J. Making sense of it all: bacterial chemotaxis. *Nat Rev Mol Cell Biol* **5,** 1024–1037 (2004) doi:10.1038/nrm1524
3. Pham, H. T., Parkinson J. S. (2011). Phenol Sensing by *Escherichia coli* Chemoreceptors: a Nonclassical Mechanism. *J. Bacteriol 193(23)*:6597-6604 doi:10/1128/JB.05987-11
4. Maddock J. R., Shapiro, L. (1993). Polar location of the chemoreceptor complex in the *Escherichia coli* cell. *Science, 259*(5102), 1717-1723. doi:10.1126/science.8456299
5. Pinas, G. E., Frank, V., Vaknin, A., Parkinson, J. S. (2016) The source of high signal cooperativity in bacterial chemosensory arrays. *Proc Natl Acad Sci U S A, 113*(12), 3335-3340. doi:10.1073/pnas.1600216113
6. Briegel, A., Li, X., Bilwes, A. M., Hughes, K. T., Jensen, G. J., & Crane, B. R., (2012) Bacterial chemoreceptor arrays are hexagonally packed trimers of receptor dimers networked by rings of kinase and coupling proteins. *Proc Natl Acad Sci U S A, 109*(10), 3766-3771. doi:10.1073/pnas.1115719109
7. Briegel, A., Ortega, D. R., Tocheva E. I., Wuichet, K., Zhuo, L., Chen, S., Muller, A., Iancu, C. V., Murphy, G. E., Dobro, M. J., Zhulin, I. B., & Jensen., G. J. (2009) Universal architecture of bacterial chemoreceptor arrays. *Proc Natl Acad Sci U S A, 106*(40) 17181-17186. doi:10.1073/pnas.095181106
8. Briegel, A., Ortega, D. R., Huang, A., Oikonomou, C. M., Gunsalus, R. P., & Jensen, G. J. (2015) Structural conservation of chemotaxis machinery across Archaea and Bacteria. *Environ Microbiol, 7*(3), 414-419. doi:10.1111/1758-2229.12265
9. Briegel, A., Ladinsky, M. S., Oikonomou, C., Jones, C. W., Harris, M, J., Fowler, D. J., Chang, Y., Thompson, L, K., Armitage, J. P. (2014) Structure of bacterial cytoplasmic chemosensory arrays and implications for chemotactic signaling. *eLife 3*(e.02151). doi:10.7554/eLife.02151
10. Wen, Y., Alvarado, A., Glatter, T., Ringaard, S., Briegel, A. (2018) Baseplate variability of *Vibrio cholerae* chemoreceptor arrays. *Proc Natl Acad Sci U S A, 115*(52) 13365-13370. doi:10.1073/pnas.1811931115
11. Briegel, A., Wong, M. L., Hodges, H. L., Oikonomou, C. M., Piasta, K. N., Harris, M. J., Fowler, D. J., Thompson, L. K., Falke, J, J., Kiessling L. L., Jensen, G. J. (2014) New insights into bacterial chemosensory array structure and assembly from electron cryotomography. *Biochem 2014*(53) 1575-1585. doi:10.1021/bi5000614
12. Cannistraro, V. J., Glekas, G. D., Rao, C. V., Ordal, G. W. (2011) Cellular stoichiometry of the chemotaxis proteins in *Bacillus subtilis*. *J Bacteriol, 193*(13) 3220-3227. doi:10.1128/JB.01255-10
13. Ringgaard, S., Yang, W., Alvarado, A., Shirner, K., Briegel, A. (2018) Chemotaxis arrays in *Vibrio* species and their intracellular positioning by the ParC/ParP System. *J Bacteriol, 200*(15). doi:10.1128/JB.00793-17

14. Huang, Z., Pan, X., Xu, N., Guo, M. (2018) Bacterial chemotaxis coupling protein: Structure, function and diversity. *Microbiol Res, 219*. doi:10.1016/j.micres.2018.11.001
15. Abedrabbo, S., Castellon, J., Collins K. D., Johnson, K. S., & Ottemann, K. M. (2017). Cooperation of two distinct coupling proteins creates chemosensory network connections. *Proc Natl Acad Sci U S A. 114*(11), 2970-2975. doi:10.1073/pnas.1618227114
16. Porter, S., Wadhams, G. & Armitage, J. (2011) Signal processing in complex chemotaxis pathways. *Nat Rev Microbiol* 9**,** 153–165 doi:10.1038/nrmicro2505
17. Pinas, G. E., DeSantis, M, D., Parkinson, J, S. (2018) Noncritical signaling role of a kinase-receptor interaction surface in the *Escherichia coli* chemosensory core complex. *J Molec Biol 430*(7) 1051-1064. doi:10.1016/j.jmb/2018/02/004
18. Fulcher, N. B., Holliday, P. M., Klem, E., Cann, M. J., & Wolfgang, M.C. (2010). The *Pseudomonas aeruginosa* Chp chemosensory system regulates intracellular cAMP levels by modulating adenylate cyclase activity. *Mol Microbiol, 76*(4), 889-904. doi:10.1111/j.126502958.2010.07135.x
19. Antibiotic Resistance Threats in the United States. (2019). U. S. Department of Health and Human Services, Centers for Disease Control and Prevention. www.cdc.gov/DrugResistance/Biggest-Threats.html
20. Bertrand, J. J., West, J. T., & Engel, J. N. (2010). Genetic analysis of the regulation of type IV pilus function by the Chp chemosensory system of *Pseudomonas aeruginosa. J Bateriol, 192*(4), 994-1010. doi:10.1128/jb/01390-09
21. Heacock-Kang, Y., Sun, Z., Zarzycki-Siek, J., McMillan, I. A., Norris, M. H., Bluhm, A. P., Cabanas, D., Fogen, D., Vo, H., Donachie, S. P., Borlee, B. R., Sibley, C.D., Lewenza, S., Schurr, M. J., Schweizer, H. P., Hoang, T. T. (2017). Spatial transcriptomes within the *Pseudomonas aeruginosa* biofilm architecture. *Mol Microbiol., 106*(6), 976-985. doi:10.1111/mmi.13863
22. Masduki A, Nakamura J, Ohga T, Umezaki R, Kato J, Ohtake H Isolation and characterization of chemotaxis mutants and genes of Pseudomonas aeruginosa. J Bacteriol 1995;177:948–52
23. Kato J, Sakai Y, Nikata T, Ohtake H Cloning and characterization of a Pseudomonas aeruginosa gene involved in the negative regulation of phosphate taxis. J Bacteriol 1994;176: 5874–7.
24. Ferrandez, A., Hawkins, A. C., Summerfiled, D. T., & Harwood, C. S. (2002) Cluster II che genes from *Pseudomonas aeruginosa* are required for an optimal chemotactic response. *J. Bacteriol, 184*(16), 4374-43383
25. Caiazza, N. C., Merritt, J. H., Brothers, K. M., O'Toole, G. A., (2007) Inverse regulation of biofilm formation and swarming motility by *Pseudomonas aeruginosa* PA14. *J. Bacteriol, 189*(9) 3603-3612. doi:10.1128/JB.01685-06
26. Whitchurch, C. B., Leech, A. J., Young, M. D., Kennedy, D., Sargent, J. L., Bertrand, J. J., Semmler, A. B., Mellick, A. S., Martin, P. R., Alm, R. A., Hobbs, M., Beatson, S. A., Huan, B., Nguyen, L., Commolli, J. C., Engel, J. N., Darzins, A., & Mattick, J. S. (2004). Characterization of a complex chemosensory signal transduction system which controls twitching motility in *Pseudomonas aeruginosa. Mol Microbiol. 52*(3), 873-893. doi:10.1111/j.136502958.2004.04026.x

27. Jansari, V. H., Potharla, V. Y., Riddell, G. T., & Bardy, S. L. (2016). Twitching motility and cAMP levels: signal transduction through a single methyl-accepting chemotaxis protein. *FEMS Microbiol Lett, 363*(12). doi:10.1093/femsle/fnw119
28. Buensuceso, R. N. C., Daniel-Ivad, M., Kilmury, S. L. N., Leighton, T. L., Harvey, H., Howell, P. L., & Burrows, L. L. (2017). Cyclic AMP-independent control of twitching motility in *Pseudomonas aeruginosa. J Bacteriol, 199*(16). doi:10.1128/jb.00188-17
29. Inclan, Y. F., Persat, A., Greninger, A., Von Dollen, J., Johnson, J., Korgan, N., Gitain, Z., & Engel, J. N. (2016). A Scaffold protein connects type IV pili with the Chp chemosensory system to mediate activation of virulence signaling in *Pseudomonas aeruginosa. Mol Microbiol, 101*(4), 590-605. doi:10.1111/mmi.13410
30. Ortega, D. R., Fleetwood, A. D., Krell, T., Harwood, C. S., Jensen, G. J., & Zhulin, I. B. (2017). Assigning chemoreceptors to chemosensory pathways in *P. aeruginosa. Proc Natl Acad Sci U S A, 114*(48), 12809-12814. doi:10.1073/pnas.1708842114
31. Silversmith, R. E., Want, B., Fulcher, N. B., Wolfgang, M. C., & Bourret, R. B. (2016). Phosphoryl group flow within the *Pseudomonas aeruginosa* Pil-Chp chemosensory system: differential function of the eight phosphotransferase and three receiver domains. *J Biol Chem, 29*(34), 17677-17691. doi:10.1074/jbc.M116.737528
32. Boukhvalova, M.S., Dahlquist, F. W., & Steward, R. C. (2002) CheW binding interactions with CheA and Tar. Importance for chemotaxis signaling in *Escherichia coli. J Biol Chem, 227*(25), 22251-22259. doi:10.1074/jbc.M110908200
33. Euromedex BACTH Kit
34. Jansari, V., (2017) The Role of PilJ and Its Structural Domains in the Localization and Function of the Chp Chemosensory System in Pseudomonas Aeruginosa. *ProQuest Dissertations and Theses*.
35. Sharma, S., (2018) Role of The Two Adaptor Proteins In The Chp Chemosensory System of *Pseudomonas aeruginosa*.
36. Hoang, T., Karkoff-Schweizer, R., Kutchmas, A., Schweizer, H. (1998). A broad-host-range Flp-*FRT* recombination system for site-specific excision of chromosomally-located DNA sequences: application for isolation of unmarked *Pseudomonas aeruginosa* mutants. *Gene, 212,* 77-86
37. Newman, J., Fuqua, C. (1999). Broad-host-range expression vectors that carry the L-arabinose-inducible *Escherichia coli* araBAD promoter and the araC regulator. *Gene 227,* 197-203
38. Ketelboeter, L. M., Bardy, S. L. (2017) Characterization of 2-(2-nitro-4-trifluoromethylbenzoyl)-1,3-cyclohexanedione resistance in pyomelanogenic *Pseudomonas aeruginosa* DKN343. *PLoS ONE 12(6):* e0178084. https://doi.org/10.1371/journal.pone.0178084
39. Faguy, D. M., D. P. Bayley, A. S. Kostyukova, N. A. Thomas, and K. F. Jarrell. (1996). Isolation and characterization of flagella and flagellin proteins from the thermoacidophilic archaea *Thermoplasma volcanium* and *Sulfolobus shibatae*. J. Bacteriol. 178**:**902-905.

40. Winsor, G. L., Griffiths, E. J., Lo R., Dhillon, B. K., Shay, J. A., Brinkman, F. S. (2016) Enhanced annotations and features for comparing thousands of *Pseudomonas* genomes in the *Pseudomonas* genome database. *Nucleic Acid Res. (2016).* Doi:10.1093/nar/gkv1227
41. Nolan, L. M., McCaughey, L. C., Merjane, J., Turnbull, L., Whitchurch, C. B. (2019). ChpC controls twitching motility-mediated expansion of *Pseudomonas aeruginosa* biofilms in response to serum albumin, mucin and oligopeptides. *bioRxiv* doi:10.1101/825596
42. Persat, A., Inclan, Y. F., Engel, J. N., Stone, H. A., Gitai, Z. (2015). Type IV pili mechanochemically regulate virulence factors in *Pseudomonas aeruginosa. Proc Natl Acad Sci U S A, 112,* 7563-7568
43. O'Neal L., Gullet M. J., Aksenova, A., Hubler, A., Briegel A., Ortega., D. Kjaer, A., Jensen, G., Alexandre, G. (2019). Distinct Chemotaxis Protein Paralogs Assemble into Chemoreceptor Signaling Arrays to Coordinate Signaling Output. *mBio* doi:10:e01757-19
44. Seitz, M. K. H., Frank, V., Massazza, D. A., Vaknin, A., Studdert, C. A. (2014). Bacterial chemoreceptors of different length classes signal independently. *Mol. Micro. 93(4)*:814-822 doi:10.1111/mmi.12700
45. Leighton, T. L., Buensuceso, R. N. C., Howell, P. L., Burrows, L. L. (2015). Biogenesis of *Pseudomonas aeruginosa* type IV pili and regulation of their function. *Env. Microbiology 17 (11),* 4148-4163
46. Corral, J., Sebastia, P., Coll, N. S., Barbe, J., Aranda, J., Valls, M. (2020). Twitching and Swimming Motility Play a Role in *Ralstonia solanacaerum* Pathogenicity. *mSphere* doi: 10.1128/mSphere.00740-19
47. Yu, C., Nguyen, D., Ren, Z., Liu, J., Yang, F., Tian, F., Fan, S., Che, H. (2020). The RpoN2-PilRX regulatory system governs type IV pilus gene transcription and is required for bacterial motility and virulence in *Xanthomonas oryzae* pv. *oryzae. Molecular Plant Pathology* doi:10.1111/mpp.12920
48. Cursino, L., Galvani, C. D., Athinuwat, D., Zaini, P. A., Li, X., De La Fuente, L., Hoch, H. C., Burr, T. J., Mowery, P. (2011). Identification of an Operon, Pil-Chp, That Controls Twitching Motility and Virulence in *Xylella fastidiosa*. *MPMI 24(10),* 1198-1206 doi:10.1094/MPMI-10-10-0252
49. Dons, L., Eriksson, E., Jin, Y., Rottenberg, M. E., Kristensson, K., Larson, C. N., Bresciani, J., Olsen, J, E. (2004). Role of Flagellin and the Two-Component CheA/CheY System of *Listeria monocytogenes* in Host Cell Invasion and Virulence. *Infection and Immunity 72(6)* : 3237-3244 doi: 10;1128/IAI.72.6.3237–3244.2004
50. Pittman, M. S., Goodwin, M., Kelly, D. J. (2001). Chemotaxis in the human gastric pathogen *Helicobacter pylori*: different roles for CheW and three CheV paralogues, and evidence for CheV2 phosphorylation. *Microbiology 147:*2493-2504 doi:
51. Huang, Z., Zhou, Q., Sun, P., Yang, J., Guo, M. (2017). Two *Agrobacterium tumefaciens* CheW proteins are incorporated into one chemosensory pathway with different efficiencies. *MPIM 31(4)*:460-4470 doi:10;1128/IAI.72.6.3237–3244.2004

52. Martin, A. C., Wadhams, G. H., Armitage, J. P. (2001). The roles of multiple CheW and CheA homologues in chemotaxis and in chemoreceptor localization in *Rhodobacter sphaeroides*. *Mol. Micro. 40(6)* : 1261-1271 doi:10.1046/j.1365-2958.2001.02468.x
53. Zhang, K., Liu, J., Tu, Y., Xu, H., Charon, N. W., Li, C. (2012) Two CheW coupling proteins are essential in a chemosensory pathway of *Borrelia burgdorferi*. *Mol. Microbiol. 85(4)*:782-794 doi:10.1111/j.1365-2958.2012.08139.x
54. Guiseppi, A., Vincente, J. J., Herrou, J., Byrne, D., Barneoud, A., Moine, A., Espinosa, L., Basse, M., Molle, V., Minot, T., Roche, P., Mauriello, E. M. F. (2019). A divergent CheW confers plasticity to nucleoid-associated chemosensory arrays. *PLoS Genet. 15(12)*:e1008533 doi:10.1371/journl.pgen.1008533
55. Wen, Y., Briegel, A. (2020). Diversity of Bacterial Chemosensory Arrays. *Trends in Microbiol. 28 (1)*: 68-80 doi:10/1016/j.tim.2019.08.002

Appendix: Supplementary Information

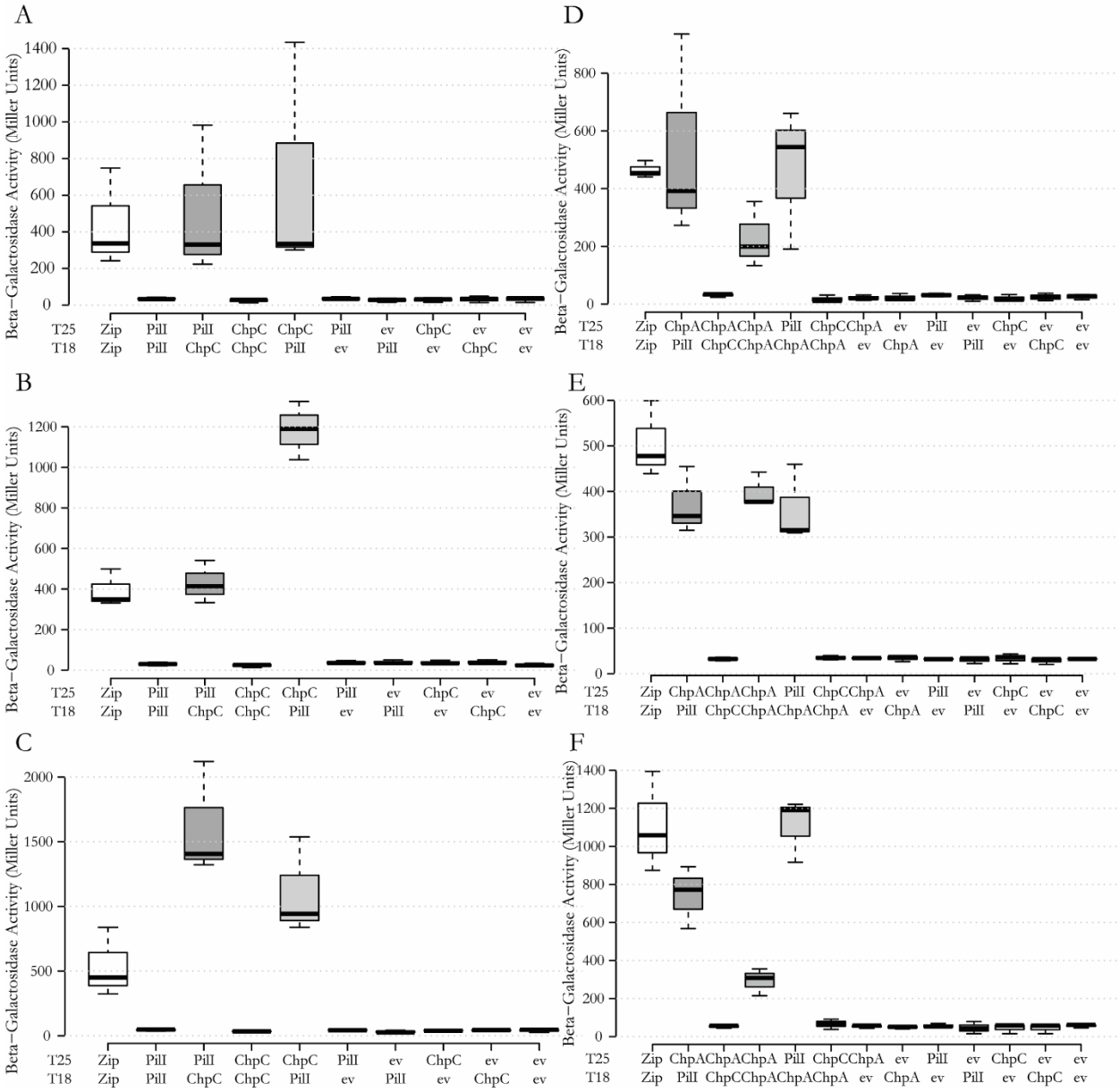

Figure S1 Bacterial Two Hybrid interaction assays for ChpA, ChpC, and PilI. Each protein of interest was fused to T25 or T18. ev indicates empty vector. β-galactosidase assays showing PilI/ChpC/ChpA interactions. PilI/ChpC and ChpC/PilI had high β-galactosidase activity compared to empty vector controls, and more consistent with the T25-Zip/T18-Zip positive control, indicating a positive interaction. PilI/PilI and ChpC/ChpC have low β-galactosidase activity consistent with empty vector controls indicating no interaction. PilI/ChpA and ChpA/PilI had high β-galactosidase activity compared to empty vector controls, and more consistent with the T25-Zip/T18-Zip positive control, indicating a positive interaction. ChpA/ChpA had high β-galactosidase activity compared to empty vector controls, and more consistent with the T25-Zip/T18-Zip positive control, indicating a positive interaction. ChpC/ChpA and ChpA/ChpC have low β-galactosidase activity consistent with empty vector controls indicating no interaction. A-B) Proteins of interest are fused to the amino terminal of both T25 and T18 C-D) Proteins of interest are fused to the carboxy terminal of T25 and the amino terminal of T18. E-F) Proteins of interest are fused to the carboxy terminal of both T25 and T18. For box plots: center lines show the medians; box limits indicate the 25th and 75th percentiles as determined by R software; whiskers extend 1.5 times the interquartile range from the 25th and 75th percentiles. n = 3 sample points. Each data point is an average of 3 technical replicates.

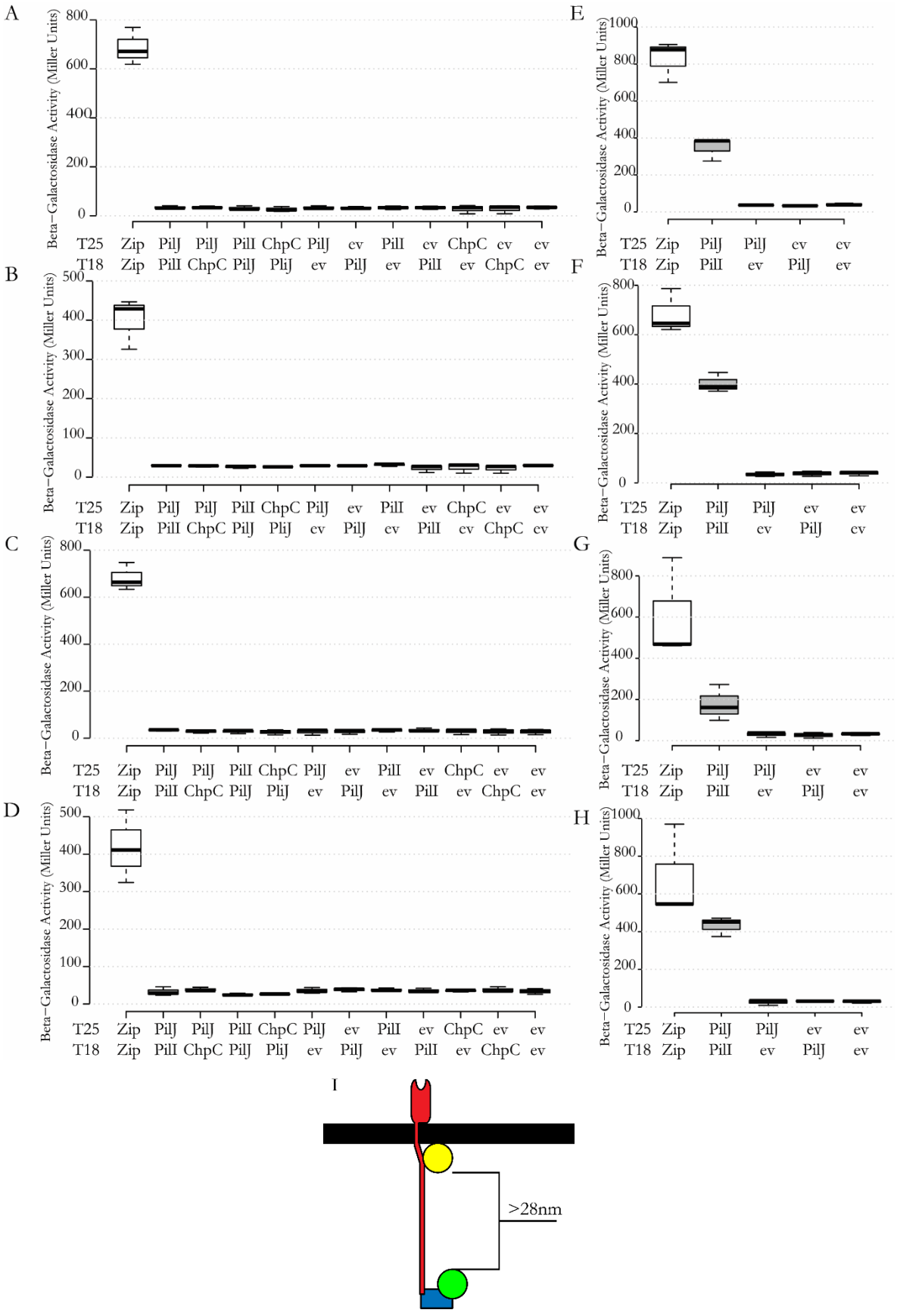
A
B
C
D
E
F
G
H
I
Beta−Galactosidase Activity (Miller Units)
T25 Zip PilJ PilJ PilI ChpC PilJ ev PilI ev ChpC ev ev
T18 Zip PilI ChpC PilJ PliJ ev PilJ ev PilI ev ChpC ev
T25 Zip PilJ PilJ ev ev
T18 Zip PilI ev PilJ ev
>28nm

Figure S2 Bacterial Two Hybrid interaction assays for PilJ, ChpC, and PilI. Each protein of interest was fused to T25 or T18. ev indicates empty vector. A-D) β-galactosidase assays showing PilI/ChpC/PilJ interactions. PilI/PilJ, PilJ/PilI, ChpC/PilJ and PilJ/ChpC have low β-galactosidase activity consistent with empty vector controls indicating no interaction. E-H) β-galactosidase assays showing PilJ/PilJ interactions. PilJ/PilJ had high β-galactosidase activity compared to empty vector controls, and more consistent with the T25-Zip/T18-Zip positive control, indicating a positive interaction. A,E)Proteins of interest are fused to the amino terminal of T25 and the carboxy terminal of T18. B,F Proteins of interest are fused to the amino terminal of both T25 and T18 C,G) Proteins of interest are fused to the carboxy terminal of T25 and the amino terminal of T18. D,H) Proteins of interest are fused to the carboxy terminal of both T25 and T18. I) Diagram showing PilJ (red) fused to T18 (Yellow) and an adaptor protein (blue) fused to T25 (green). The predicted interaction at the tip of the cytoplasmic domain of PilJ is shown. Spacing between T25 and T18 fragments is shown. For box plots: center lines show the medians; box limits indicate the 25th and 75th percentiles as determined by R software; whiskers extend 1.5 times the interquartile range from the 25th and 75th percentiles. n = 3 sample points. Each data point is an average of 3 technical replicates.

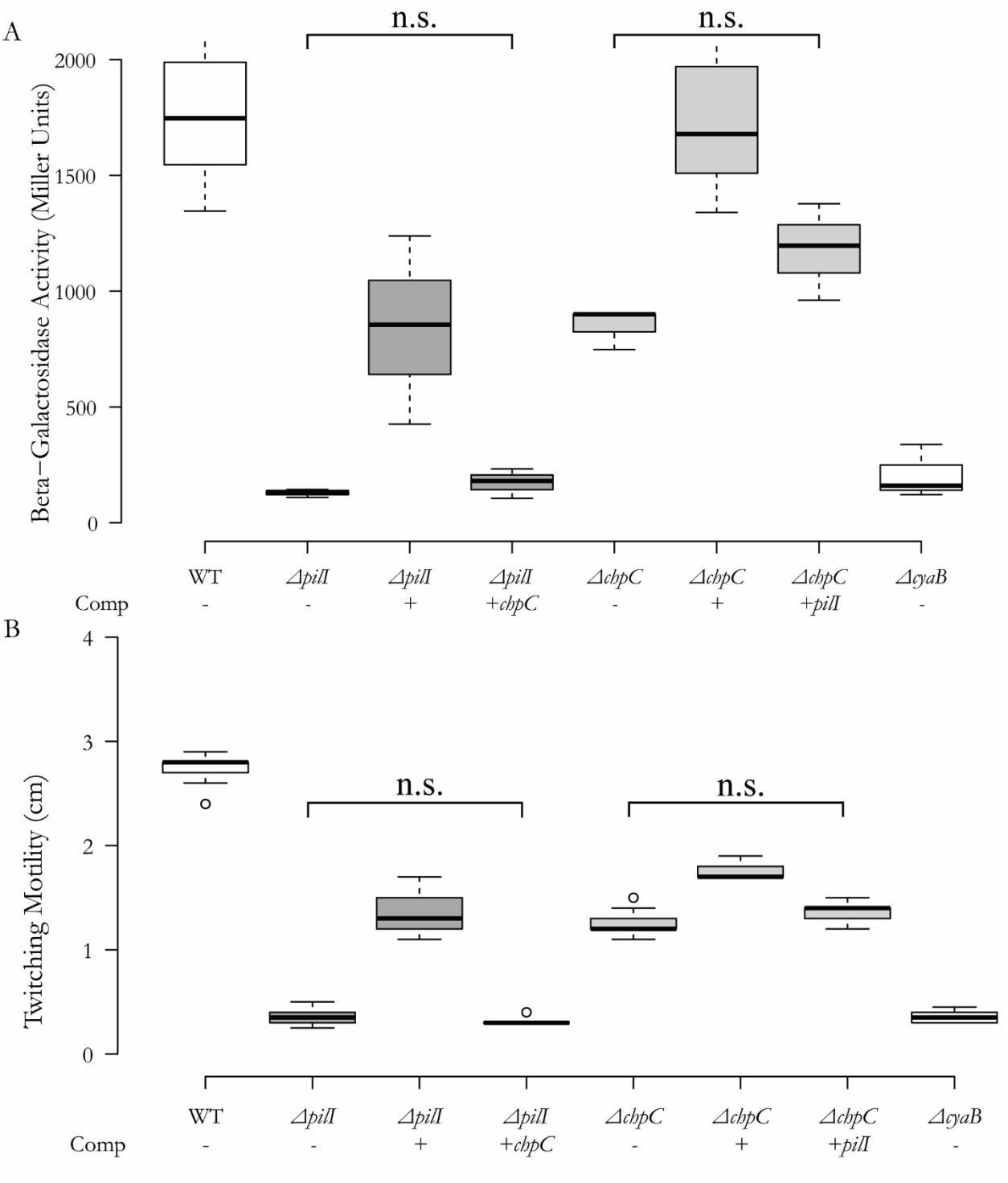
A
n.s.
n.s.
Beta−Galactosidase Activity (Miller Units)
2000
1500
1000
500
0
WT
ΔpilI
ΔpilI
ΔpilI
ΔchpC
ΔchpC
ΔchpC
ΔcyaB
Comp
-
-
+
+chpC
-
+
+pilI
-
B
n.s.
n.s.
Twitching Motility (cm)
4
3
2
1
0
WT
ΔpilI
ΔpilI
ΔpilI
ΔchpC
ΔchpC
ΔchpC
ΔcyaB
Comp
-
-
+
+chpC
-
+
+pilI
-

Figure S3 Complementation of *ΔpilI* with *chpC* or *ΔchpC* with *pilI* does not affect phenotype. A) Indicated strains were assayed for β-galactosidase activity, an indicator of intracellular cAMP bound to Vfr. Center lines show the medians; box limits indicate the 25th and 75th percentiles as determined by R software; whiskers extend 1.5 times the interquartile range from the 25th and 75th percentiles. n = 3 sample points. Each data point is an average of 3 technical replicates. B) Twitching motility of the indicated strains as determined by the diameter of the twitching motility zones. Center lines show the medians; box limits indicate the 25th and 75th percentiles as determined by R software; whiskers extend 1.5 times the interquartile range from the 25th and 75th percentiles, outliers are represented by dots. n = 9 colonies. n.s. indicates an insignificant difference $p>0.05$.

Table S1: Bacterial Two-Hybrid *E. coli* DHM1 Strains

Experimental Strains		
pUT18(C) Plasmid	pK(N)T25 Plasmid	Source
pUT18:*chpC*	pKT25:*chpC*	This Study
pUT18:*chpC*	pKT25:*pilI*	This Study
pUT18:*chpC*	pKT25:*chpA* $_{AA1668\text{-}2349}$	This Study
pUT18:*chpC*	pKNT25:*chpC*	[35]
pUT18:*chpC*	pKNT25:*pilI*	[35]
pUT18:*chpC*	pKNT25:*chpA* $_{AA1668\text{-}2349}$	This Study
pUT18:*pilI*	pKT25:*pilI*	This Study
pUT18:*pilI*	pKT25:*chpC*	This Study
pUT18:*pilI*	pKT25:*chpA* $_{AA1668\text{-}2349}$	This Study
pUT18:*pilI*	pKNT25:*pilI*	[35]
pUT18:*pilI*	pKNT25:*chpC*	[35]
pUT18:*pilI*	pKNT25:*chpA* $_{AA1668\text{-}2349}$	This Study
pUT18:*chpA* $_{AA1668\text{-}2349}$	pKT25:*chpA* $_{AA1668\text{-}2349}$	This Study
pUT18:*chpA* $_{AA1668\text{-}2349}$	pKT25:*pilI*	This Study
pUT18:*chpA* $_{AA1668\text{-}2349}$	pKT25:*chpC*	This Study
pUT18:*chpA* $_{AA1668\text{-}2349}$	pKNT25:*chpA* $_{AA1668\text{-}2349}$	This Study
pUT18:*chpA* $_{AA1668\text{-}2349}$	pKNT25:*pilI*	This Study
pUT18:*chpA* $_{AA1668\text{-}2349}$	pKNT25:*chpC*	This Study
pUT18C:*chpC*	pKT25:*chpC*	This Study
pUT18C:*chpC*	pKT25:*pilI*	This Study
pUT18C:*chpC*	pKT25:*chpA* $_{AA1668\text{-}2349}$	This Study

pUT18C:*chpC*	pKNT25:*chpC*	This Study
pUT18C:*chpC*	pKNT25:*pilI*	This Study
pUT18C:*chpC*	pKNT25:*chpA* $_{AA1668\text{-}2349}$	This Study
pUT18C:*pilI*	pKT25:*pilI*	This Study
pUT18C:*pilI*	pKT25:*chpC*	This Study
pUT18C:*pilI*	pKT25:*chpA* $_{AA1668\text{-}2349}$	This Study
pUT18C:*pilI*	pKNT25:*pilI*	This Study
pUT18C:*pilI*	pKNT25:*chpC*	This Study
pUT18C:*pilI*	pKNT25:*chpA* $_{AA1668\text{-}2349}$	This Study
pUT18C:*chpA* $_{AA1668\text{-}2349}$	pKT25:*chpA* $_{AA1668\text{-}2349}$	This Study
pUT18C:*chpA* $_{AA1668\text{-}2349}$	pKT25:*pilI*	This Study
pUT18C:*chpA* $_{AA1668\text{-}2349}$	pKT25:*chpC*	This Study
pUT18C:*chpA* $_{AA1668\text{-}2349}$	pKNT25:*chpA* $_{AA1668\text{-}2349}$	This Study
pUT18C:*chpA* $_{AA1668\text{-}2349}$	pKNT25:*pilI*	This Study
pUT18C:*chpA* $_{AA1668\text{-}2349}$	pKNT25:*chpC*	This Study
Control Strains		
pUT18(C) Plasmid	pK(N)T25 Plasmid	Source
pUT18:*chpC*	pKT25	This Study
pUT18:*chpC*	pKNT25	This Study
pUT18:*pilI*	pKT25	This Study
pUT18:*pilI*	pKNT25	This Study
pUT18:*chpA* $_{AA1668\text{-}2349}$	pKT25	This Study
pUT18:*chpA* $_{AA1668\text{-}2349}$	pKNT25	This Study
pUT18C:*chpC*	pKT25	[35]

pUT18C:*chpC*	pKNT25	This Study
pUT18C:*pilI*	pKT25	[35]
pUT18C:*pilI*	pKNT25	This Study
pUT18C:*chpA* $_{AA1668\text{-}2349}$	pKT25	This Study
pUT18C:*chpA* $_{AA1668\text{-}2349}$	pKNT25	This Study
pUT18	pKT25:*pilI*	This Study
pUT18	pKT25:*chpC*	This Study
pUT18	pKT25:*chpA* $_{AA1668\text{-}2349}$	This Study
pUT18	pKNT25:*pilI*	[35]
pUT18	pKNT25:*chpC*	[35]
pUT18	pKNT25:*chpA* $_{AA1668\text{-}2349}$	This Study
pUT18C	pKT25:*pilI*	This Study
pUT18C	pKT25:*chpC*	This Study
pUT18C	pKT25:*chpA* $_{AA1668\text{-}2349}$	This Study
pUT18C	pKNT25:*pilI*	This Study
pUT18C	pKNT25:*chpC*	This Study
pUT18C	pKNT25:*chpA* $_{AA1668\text{-}2349}$	This Study
pUT18	pKT25	This Study
pUT18	pKNT25	[35]
pUT18C	pKT25	This Study
pUT18C	pKNT25	This Study
pUT18C-zip	pKT25-zip	[35]